ARTICLE

Bcl-6 expression by CD4$^+$ T cells determines concomitant immunity and host resistance across distinct parasitic infections

Alexandre P. Meli [1,2,†], Gabriel A. Russell [1,2,†], Sharada Swaminathan [3,✉], Laura Weichselbaum [4], Clara A. MacMahon [1,2], Erwan Pernet [5], Danielle Karo-Atar [1,2], Dakota Rogers [6], Annie Rochette [7], Ghislaine Fontes [1,2], Judith N. Mandl [2,6], Maziar Divangahi [5], Ophir D. Klein [4,8], Alex Gregorieff [7,9], Simona Stäger [3,‡] and Irah L. King [1,2,9,10,✉,‡]

Cluster of differentiation (CD4$^+$) T cells consist of multiple subtypes, defined by expression of lineage-specific transcription factors, that contribute to the control of infectious diseases by providing help to immune and nonimmune target cells. In the current study, we examined the role of B cell lymphoma (Bcl)-6, a transcriptional repressor and master regulator of T follicular helper cell differentiation, in T cell-mediated host defense against intestinal and systemic parasitic infections. We demonstrate that while Bcl-6 expression by CD4$^+$ T cells is critical for antibody-mediated protective immunity against secondary infection with the nematode *Heligmosoides polygyrus bakeri*, it paradoxically compromises worm expulsion during primary infection by limiting the generation of interleukin-10 (IL-10)-producing Gata3$^+$ T helper 2 cells. Enhanced worm expulsion in the absence of Bcl-6 expressing T cells was associated with amplified intestinal goblet cell differentiation and increased generation of alternatively activated macrophages, effects that were reversed by neutralization of IL-10 signals. An increase in IL-10 production by Bcl-6-deficient CD4$^+$ T cells was also evident in the context of systemic *Leishmania donovani* infection, but in contrast to *Heligmosoides polygyrus bakeri* infection, compromised T helper 1-mediated liver macrophage activation and increased susceptibility to this distinct parasitic challenge. Collectively, our studies suggest that host defense pathways that protect against parasite superinfection and lethal systemic protozoal infections can be engaged at the cost of compromised primary resistance to well-tolerated helminths.

Mucosal Immunology (2023) 16:801–816; https://doi.org/10.1016/j.mucimm.2023.08.004

INTRODUCTION

Cluster of differentiation (CD4$^+$) T effector cells are commonly segregated based on the expression of lineage-specific transcription factors that endow each subset with a specific cytokine secretion profile[1]. In the context of helminth infection or allergic immunity, T helper (Th)2 cells expressing the transcription factor Gata-3 predominate and produce interleukin (IL)-4, IL-5, and IL-13 within mucosal tissues. However, we now know that this paradigm is an oversimplification, prompting some to suggest a more function-based delineation of T helper subsets[2]. Indeed, we and others have shown that Bcl-6 expressing T follicular helper (Tfh) cells, which mediate diverse forms of humoral immunity, are potent producers of IL-4 and IL-13 despite minimal expression of Gata-3[3–5]. Similarly, IL-10, first identified as a Th2 cytokine, was recently implicated in expulsion of parasitic worms[6,7]. Nevertheless, IL-10 can be produced by a multitude of other Th effector subsets, including T-bet$^+$ Th1, Rorgt$^+$ Th17, and Foxp3$^+$ T regulatory (Treg) cells, and have unique effects of immunoregulation. Thus, the context must be considered when defining how lineage-specific transcription factors impact the cytokine profiles of T effector subsets and their impact on host defense.

Infection of mice with the roundworm *Heligmosomoides polygyrus bakeri* (*Hpb*) induces a robust Th2 and Tfh cell response that mediate distinct yet complementary roles in parasite expulsion[8]. Following dendritic cell-mediated priming in the gut-draining mesenteric lymph nodes (mesLNs) and re-encounter with cognate antigen following migration to the small intestine (SI), IL-4 and IL-13-producing Th2 cells drive worm expulsion through increased epithelial cell turnover and goblet cell secretion of mucus, the so-called "weep and sweep" response of the intestinal epithelium[9,10]. In a complementary fashion, Tfh cells localize to B cell follicles, where they promote class-switching and affinity maturation of germinal center (GC) B cells and the production of antigen-specific antibodies. As such, *Hpb* infection provides a unique setting to investigate molecular pathways

[1]Department of Microbiology and Immunology, Meakins-Christie Laboratories, Research Institute of the McGill University Health Centre, Montreal, Quebec, Canada. [2]McGill Interdisciplinary Initiative in Infection and Immunity, Montreal, Quebec, Canada. [3]Institut Armand Frappier, Laval, Quebec, Canada. [4]Department of Orofacial Sciences and Program in Craniofacial Biology, University of California, San Francisco, San Francisco, CA, USA. [5]Research Institute of the McGill University Health Centre, Meakins-Christie Laboratories, Department of Medicine, Montreal, Quebec, Canada. [6]Department of Physiology and McGill Research Centre for Complex Traits, McGill University, Montreal, Quebec, Canada. [7]Department of Pathology and Cancer Research Program, McGill University, Montreal, Quebec, Canada. [8]Department of Pediatrics, Cedars-Sinai Medical Center, Los Angeles, CA, USA. [9]McGill Regenerative Medicine Network, Montreal, Quebec, Canada. [10]McGill Centre for Microbiome Research, Montreal, Quebec, Canada. ✉email: irah.king@mcgill.ca

Received: 23 March 2023 Revised: 3 August 2023 Accepted 28 August 2023
Published online: 20 September 2023

that regulate the differentiation and function of these two effector cell subsets. Unlike primary infection, protection against secondary *Hpb* challenge has been shown to depend on the production of parasite-specific immunoglobulin G (IgG)1 antibody[11], which mediates the entrapment of invading larvae by alternatively activated macrophages (AAMs), preventing their maturation into adult worms[12]. Given their role in licensing antibody class-switching, Tfh cells are thus assumed to be essential for this process, though an explicit requirement for this cell type in secondary *Hpb* infection has never been directly assessed.

The differentiation of $CD4^+$ T cells into effector lineages is a tightly regulated process that requires a balance between a multitude of transcription factor-dependent signaling pathways. Of particular interest is Bcl-6, a transcriptional repressor not only required for Tfh cell differentiation but also expressed by other effector lineages[13–15]. Bcl-6 has also been shown to regulate IL-4-driven signal transducer and activator of transcription (STAT)6 target genes, including Gata-3[16], in addition to the production of IL-4 and IL-13[17] required for Th2 cell lineage commitment and effector function. However, recent studies in models of allergy and helminth infection suggest that the impact of Bcl-6 on canonical Th2 differentiation may be T cell-extrinsic[4,18]. Given the seemingly complementary roles that Tfh and Th2 cells play in host defense against *Hpb* infection, we examined how Bcl-6 directly regulates $CD4^+$ T cell function in this context and its downstream effects on innate immune cell function. Herein, we demonstrate that Bcl-6 expression by $CD4^+$ T cells enhanced host resistance to primary *Hpb* infection but was required for humoral immunity to secondary infection as well as concomitant immunity (i.e. protection against superinfection) against the same parasite. These disparate effects of Bcl-6 on host defense were due to its simultaneous impact on Tfh cell-dependent humoral immunity as well as regulation of IL-10 production by Th2 cells. Importantly, the function of this transcriptional repressor was conserved across $CD4^+$ T effector lineages, as Bcl-6 also limited IL-10 production by Th1 cells and, as a result, compromised host resistance to *Leishmania donovani* (*Ld*) infection. Overall, our studies reveal a context-dependent role for Bcl-6 in $CD4^+$ T cell-mediated host defense and the need for a diverse T effector cell response to combat distinct parasite infections.

RESULTS

Bcl-6 expression by T cells is required for protective humoral immunity to *Hpb* infection and prevention of superinfection

To determine whether Bcl-6 expression by $CD4^+$ T cells contributes to protective humoral immunity during parasite infection, we infected CD4cre-$Bcl6^{fl/fl}$ mice crossed to our IL-4 dual-reporter line (hereafter referred to as 4get/KN2.$T^{\Delta Bcl6}$ mice) that we have previously described[4] with *Hpb* (infection protocol depicted in Fig. 1A). Following gavage, *Hpb* larvae encyst in the duodenal submucosa to emerge and persist in the small intestinal lumen as adult worms, beginning at 8-10 days postinfection. *Hpb* infection of 4get/KN2.$T^{\Delta Bcl6}$ mice results in the complete abrogation of Tfh and GC B cell responses, while the generation of Gata-3^+ Th2 cells is unaltered compared to littermate controls[4]. To further characterize the contribution of Bcl-6 in $CD4^+$ T cell-dependent humoral immunity against this parasitic helminth, we examined the ability of 4get/KN2.$T^{\Delta Bcl6}$ mice to generate protective, parasite-specific antibody responses in primary versus secondary infection (experimental design depicted in Fig. 1A). Consistent with an impaired GC response, 4get/KN2.$T^{\Delta Bcl6}$ mice produced significantly less *Hpb*-specific IgG1 during primary infection compared to 4get/KN2.T^{WT} littermate controls (Fig. 1B). These differences were even greater after secondary infection, as mice cured of *Hpb* using an anthelmintic and then reinfected displayed amplified differences in parasite-specific IgG1 titers (Fig. 1C). Since the generation of *Hpb*-specific IgG1 is required for protection against reinfection[11], we measured adult worm burden and fecal egg counts 14 days after secondary infection. As expected, the small intestine of 4get/KN2.$T^{\Delta Bcl6}$ mice contained significantly more adult *Hpb* and fecal egg counts compared to 4get/KN2.T^{WT} mice during secondary challenge (Figs. 1D and 1E). We next tested whether the failure of 4get/KN2.$T^{\Delta Bcl6}$ mice to generate humoral immunity to *Hpb* infection would also render these animals susceptible to superinfection. Indeed, it has been shown in settings of *Leishmania major*[19] and *Schistosoma mansoni*[20] infections that persistent infection protects the host from subsequent infection with the same parasite, a phenomenon known as concomitant immunity. To this end, mice were reinfected with *Hpb* larvae 6 weeks after primary infection without prior administration of anthelmintics (Fig. 1F). Whereas littermate controls were protected from reinfection (as determined by no change in egg counts upon secondary infection), the feces of 4get/KN2.$T^{\Delta Bcl6}$ mice harbored significantly elevated fecal egg counts upon superinfection (Fig. 1G). Collectively, these results demonstrate that the absence of Bcl-6^+ T cells is crucial for humoral responses and concomitant immunity to *Hpb* infection.

Although our initial studies did not reveal a difference between groups in worm burden or parasite fecundity at 2 weeks postinfection (Figs. 1D and 1E), assessment of worm and egg burden at 4 weeks post-infection revealed that, despite an inability to mount protective humoral responses to secondary or superinfection, 4get/KN2.$T^{\Delta Bcl6}$ mice unexpectedly displayed increased resistance to primary *Hpb* infection (Figs. 1H and 1I). As we have previously shown that deletion of Bcl-6 in T cells results in a failure to generate a GC response, we questioned whether altered B cell differentiation may indirectly affect T cell functionality and contribute to enhanced worm expulsion. To test this possibility, we infected Mb1-cre mice crossed to our $Bcl6^{fl/fl}$ line to delete Bcl-6 in the B cell lineage (4get/KN2.$B^{\Delta Bcl6}$ mice). While we have previously shown that these mice also fail to generate a GC response[4], neither worm burden nor fecundity were significantly different at 4 weeks post-infection compared to littermate control mice (Figs. 1J and 1K). These results suggested that accelerated worm expulsion in 4get/KN2.$T^{\Delta Bcl6}$ mice during primary infection was mediated through $CD4^+$ T cell-intrinsic mechanisms. We confirmed this observation using a previously published $CD4^+$ T cell adoptive transfer approach[10]. Specifically, $CD4^+$ T cells were isolated from 4get/KN2.T^{WT} or 4get/KN2.$T^{\Delta Bcl6}$ mice at 2 weeks post-*Hpb* infection and intravenously transferred into WT mice that had been infected 7 days prior. Despite the presence of an endogenous $CD4^+$ T cell population in the recipient mice, the transfer of Bcl-6-deficient $CD4^+$ T cells resulted in increased adult worm expulsion at 4 weeks post-infection compared to the transfer of Bcl-6-sufficient $CD4^+$ T cells (Figs. 1L and 1M). Therefore, Bcl-6 deletion in $CD4^+$ T cells is sufficient to enhance *Hpb* clearance by the host.

Bcl-6 limits the generation of IL-10-producing Th2 cells during *Hpb* infection

We next sought to understand the mechanism by which Bcl-6 enhanced the anti-helminth activity of $CD4^+$ T cells, independent

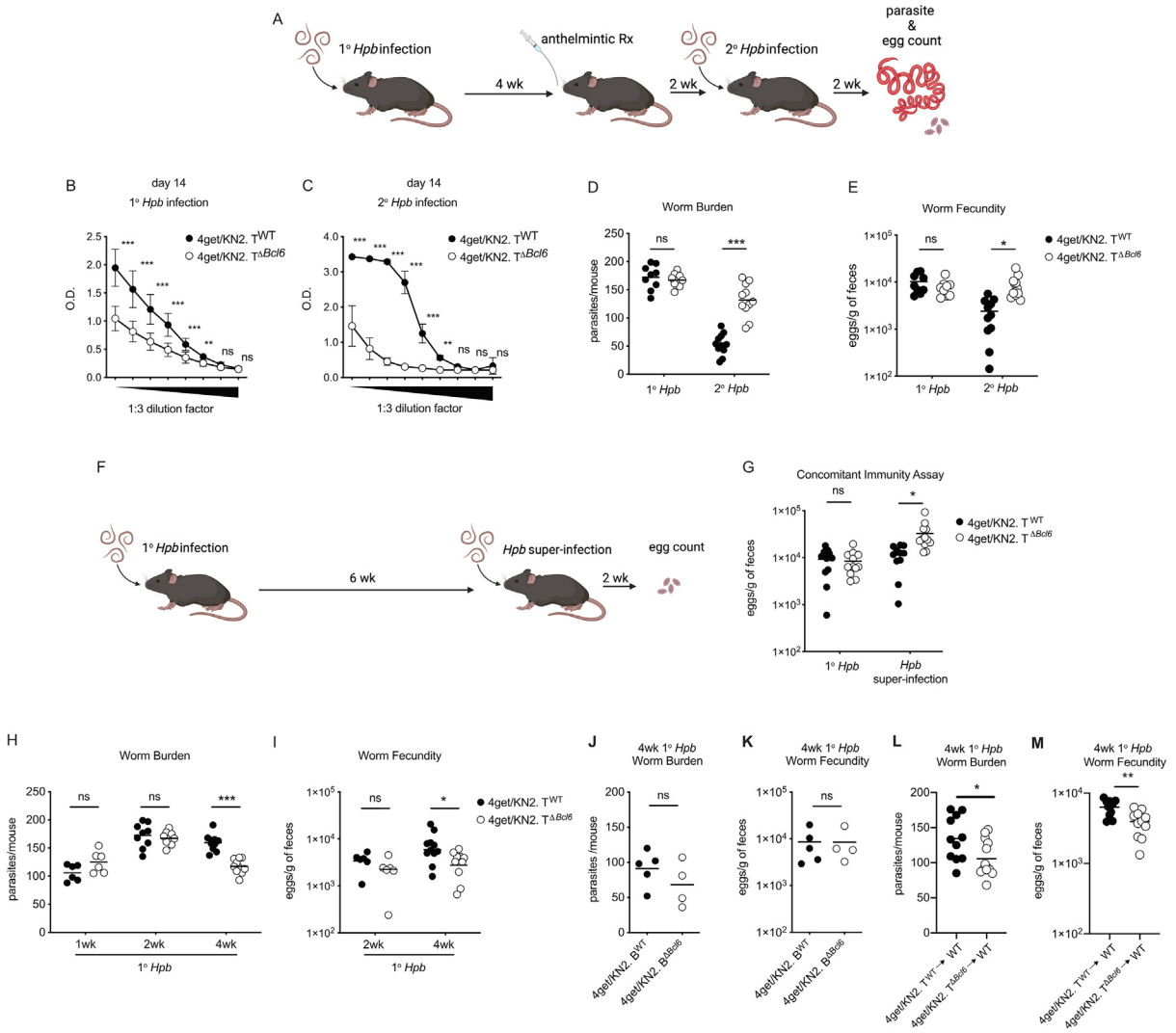

Fig. 1 Bcl-6 expression by T cells is required for protective humoral immunity to *Hpb* infection and prevention of superinfection. (A) Experimental scheme for (B–E). Mice were infected with 200 L3 infective larvae by gavage. *Hpb* excretory-secretory protein (HES)-specific IgG1 from the serum of 4get/KN2.T$^{\Delta WT}$ and 4get/KN2.T$^{\Delta Bcl6}$ mice at (B) 2 weeks after primary infection and (C) 2 weeks after secondary infection of cured mice. (D) Worm burden and (E) fecundity 2 weeks post-primary infection or 2 weeks post-secondary infection of cured mice. (F) Experimental scheme for (G). (G) Worm fecundity of 4get/KN2.T$^{\Delta WT}$ and 4get/KN2.T$^{\Delta Bcl6}$ mice during primary infection and after reinfection. Reinfected mice were infected with 200 L3 larvae at 6 weeks after primary infection (without cure), and fecundity was assayed at two weeks following secondary challenge. (H) Worm burden and (I) fecundity during primary infection at the time points indicated. 4get/KN2.B$^{\Delta WT}$ and 4get/KN2.B$^{\Delta Bcl6}$ mouse (J) worm burden and (K) fecundity 4 weeks post-*Hpb* infection. (L and M) 4get/KN2.T$^{\Delta WT}$ and 4get/KN2.T$^{\Delta Bcl6}$ mice were infected with 200 L3 *Hpb* larvae, and CD4$^+$ T cells were isolated from the mesenteric lymph nodes at 2 weeks post-infection. 4×10^6 cells were transferred intravenously into recipient mice, and 3 weeks post-transfer (4 weeks post-*Hpb* infection), intestinal worm burden (L) and fecundity (M) were assessed. (B, C, J, and K) Data are representative of at least two independent experiments with at least four mice per group. (D–I, L, and M) Data are pooled from two to three independent experiment with at least three mice per group. Data were analyzed by two-tailed Student's t test unless otherwise stated. One-way ANOVA was used in (D–G, H, and I). Dots in graphs represent individual mice. ***$p < 0.001$, **$p < 0.01$, and *$p < 0.05$. Error bars, SD; ns, not significant. (A and D) Images were created using BioRender.com. ANOVA = analysis of variance; *Hpb* = *Heligmosomoides polygyrus bakeri*.

of humoral immunity. Although it is well-established that Th2 cells uniquely contribute to *Hpb* immunity[10], our previous results demonstrated that intrinsic deletion of Bcl-6 in CD4$^+$ cells did not impact Th2 cell differentiation nor their production of IL-4 and IL-13 in this setting[4]. To investigate potential noncanonical effectors of Th2 cells, we performed bulk RNA sequencing on purified CD4$^+$CD44$^+$CXCR5$^-$IL-4 expressing [green fluorescent protein (GFP)$^+$] Th2 effector cells at two weeks post-infection (Fig. 2A). Bcl-6 deletion resulted in the significant upregulation of 157 genes and significant downregulation of 115 genes (Fig. 2B). Bcl-6 has been reported to critically mediate CD4$^+$ T cell differentiation by repressing networks of gene promoters and

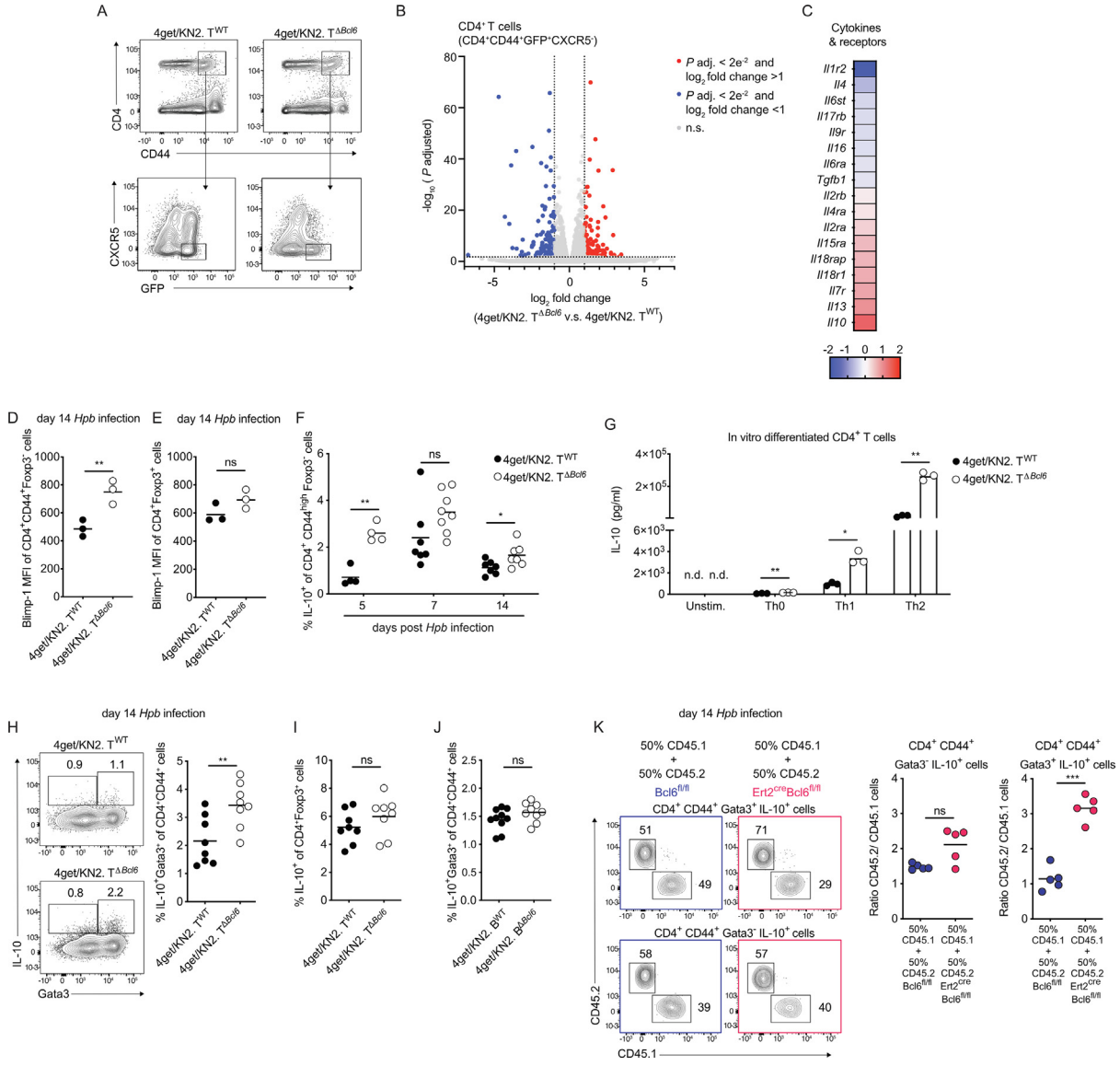

Fig. 2 Bcl-6 limits the generation of IL-10-producing Th2 cells during *Hpb* infection. (A) Representative gating strategy for sorting $CD4^+CD44^+GFP^+CXCR5^-$ mesLN cells at two weeks post-*Hpb* infection for RNA sequencing. (B) Volcano plot representing genes differentially regulated at least 1-fold in $CD4^+GFP^+CD44^+CXCR5^-$ cells from *Hpb*-infected 4get/KN2.$T^{\Delta Bcl6}$ mice compared to cells from *Hpb*-infected 4get/KN2.$T^{\Delta WT}$ controls, as determined by RNAseq. (C) Heat map of differentially expressed genes related to cytokines and associated receptors from (A). Blimp-1 expression by $CD4^+CD44^+Foxp3^-$ T cells (D) and $CD4^+CD44^+Foxp3^+$ T cells (E) from 2-week *Hpb*-infected mice. (F) Frequencies of IL-10-producing $Foxp3^-CD44^+CD4^+$ cells at various time points post-*Hpb* infection. (G) Concentration of IL-10 in the supernatant of naive $CD4^+CD62L^+$ T cells from 4get/KN2.$T^{\Delta Bcl6}$ and 4get/KN2.$T^{\Delta WT}$ littermate controls cultured under Th0, Th1, or Th2 skewing conditions for 96 hours. (H and I) Representative contour plots and frequency of (H) $Gata3^+CD44^+CD4^+$ and (I) $CD4^+Foxp3^+$ IL-10-producing T cells at 2 weeks post-*Hpb* infection. (J) Frequency of $Gata3^+CD44^+CD4^+$ IL-10-producing cells from 4get/KN2.$B^{\Delta WT}$ and 4get/KN2.$B^{\Delta Bcl6}$ mice. (K) 12 weeks after reconstitution, chimeras were treated with two consecutive doses of tamoxifen (5 mg) by gavage, infected with *Hpb* 1-week post-tamoxifen administration, and mesLNs were harvested 2 weeks post-infection. Representative expression of CD45.1 and CD45.2 by mesLN $IL\text{-}10^+Gata3^-CD44^+CD4^+$ and $IL\text{-}10^+Gata3^+CD44^+CD4^+$ cells and the ratio of the frequency of $CD45.2^+$ to $CD45.1^+$ IL-10-producing $Gata3^-CD44^+CD4^+$ or $Gata3^+CD44^+CD4^+$ cells. (A–C) Representative of one experiment with two mice per group. (D, E, G, and K) Representative of two independent experiments with at least three mice per group. (F) Data compiled from five independent experiments with at least three mice per group. (H–J) Data shown are pooled from two independent experiments with at least four mice per group. Data were analyzed by two-tailed Student's t test unless otherwise stated. Dots in graphs represent individual mice. ***$p < 0.001$, **$p < 0.01$, and *$p < 0.05$. ns, not significant. *Hpb* = *Heligmosomoides polygyrus bakeri*; IL = interleukin; mesLN = mesenteric lymph node; RNAseq = RNA sequencing; Th = T helper.

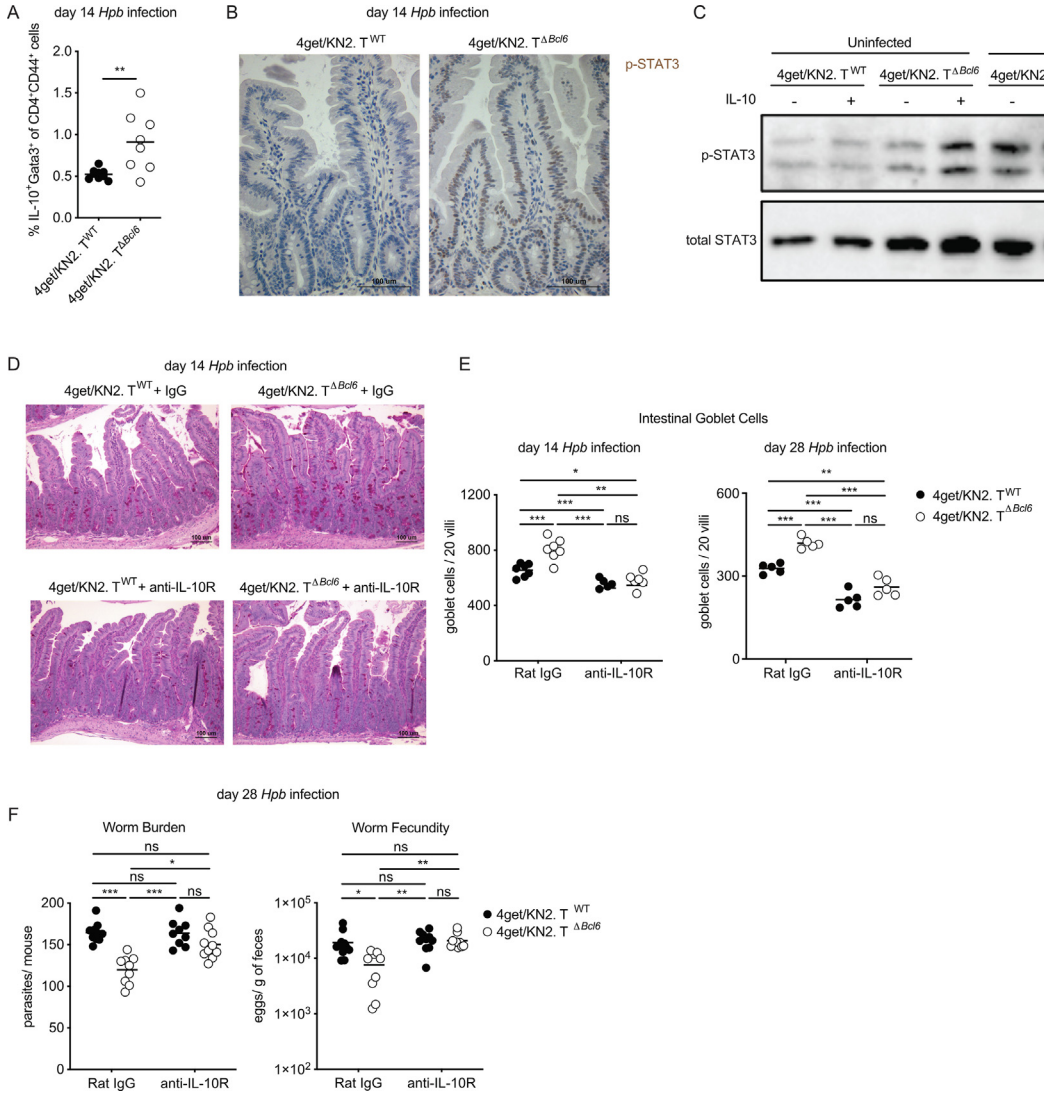

Fig. 3 IL-10 signaling enhances type 2 cytokine-dependent goblet cell differentiation and *Hpb* expulsion. (A) Frequency of small intestinal Gata3^{+}CD44^{+}CD4^{+} IL-10-producing T cells from 2-week *Hpb*-infected mice. (B) Representative images of duodenum from 2-week *Hpb*-infected 4get/KN2.T$^{\Delta WT}$ and 4get/KN2.T$^{\Delta Bcl6}$ mice stained by immunohistochemistry for phosphorylated STAT3 (residue Tyr705). Images are representative of two independent experiments with at least three mice per group. (C) Immunoblot of p-STAT3 and total STAT3 from small intestinal crypts were generated from uninfected or 2-week *Hpb*-infected 4get/KN2.T$^{\Delta WT}$ and 4get/KN2.T$^{\Delta Bcl6}$ mice and stimulated for 30 minutes with 10 ng/ml of IL-10. (D and E) 4get/KN2.T$^{\Delta WT}$ and 4get/KN2.T$^{\Delta Bcl6}$ mice were treated with anti-IL-10R or isotype control every 3 days from the start of *Hpb* infection. Representative P.A.S stained images (D) and enumeration (E) of goblet cells from duodenal sections isolated from 2- and 4-week *Hpb*-infected mice. (F) Intestinal worm burden and parasite fecundity at 4 weeks post-*Hpb* infection. (A, E, and F) Compiled from two independent experiments with at least three mice per group. (B–D) Representative of two independent experiments with at least four mice per group. Dots in graphs represent individual mice. Data were analyzed by 2-tailed Student's t test in (A) and one-way ANOVA in (E and F). ***$p < 0.001$, **$p < 0.01$, and *$p < 0.05$. ns, not significant. ANOVA = analysis of variance; *Hpb* = *Heligmosomoides polygyrus bakeri*; IL = interleukin; IL-10R, IL-10 receptor; P.A.S = Periodic Acid Schiff; p-STAT = phosphorylated STAT; STAT = signal transducer and activator of transcription.

enhancers[21]. The expression of Bcl-6 itself can also be regulated by the transcriptional repressor Blimp-1[13]. While not mutually exclusive, there is a negative correlation between levels of Bcl-6 and Blimp-1 expression in CD4^{+} T cell effector lineages[13]. Consistent with this literature, *Prdm1*, the gene coding for Blimp-1, was significantly upregulated in Bcl-6-deficient Th2 effector cells (complete gene list can be found at http://www.ncbi.nlm.nih.gov/bioproject/940100; Supplementary Table 1). As the Bcl-6/Blimp-1 axis has also been reported to regulate IL-10 production[18,22], *Il10* mRNA was the most significantly increased cytokine detected in Bcl-6-deficient Th2 cells compared to controls (Fig. 2C). To confirm the impact of Bcl-6 deficiency on this network *in vivo*, we first evaluated CD4^{+} T cell expression of Blimp-1 at 2 weeks post-*Hpb* infection. Indeed, activated

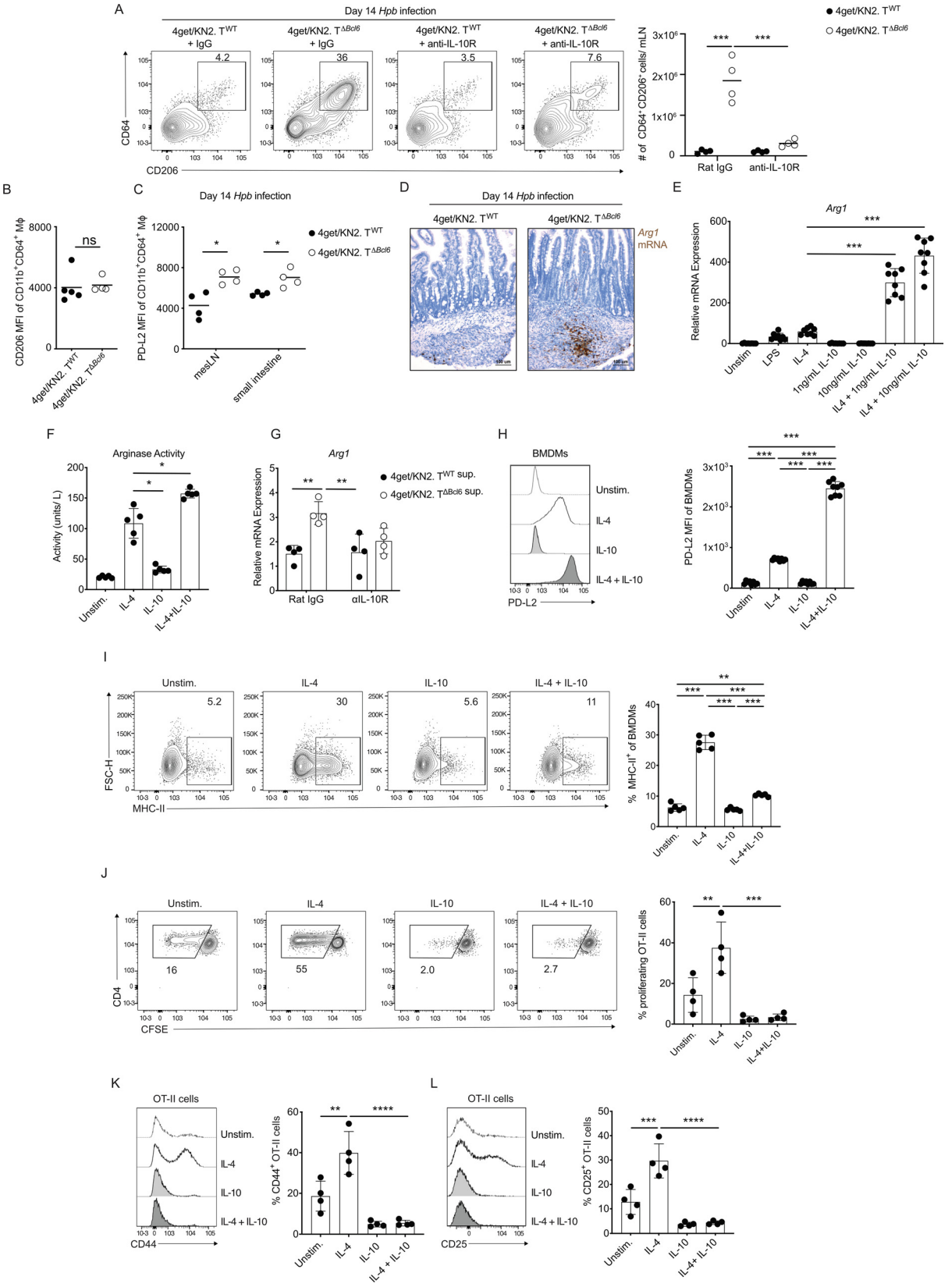
A
Day 14 Hpb infection
4get/KN2. TWT + IgG
4get/KN2. TΔBcl6 + IgG
4get/KN2. TWT + anti-IL-10R
4get/KN2. TΔBcl6 + anti-IL-10R
4.2
36
3.5
7.6
CD64
CD206
4get/KN2. TWT
4get/KN2. TΔBcl6
# of CD64+ CD206+ cells/ mLN
Rat IgG
anti-IL-10R
B
CD206 MFI of CD11b+CD64+ Mφ
ns
4get/KN2. TWT
4get/KN2. TΔBcl6
C
Day 14 Hpb infection
PD-L2 MFI of CD11b+CD64+ Mφ
mesLN
small intestine
D
Day 14 Hpb infection
4get/KN2. TWT
4get/KN2. TΔBcl6
Arg1 mRNA
E
Arg1
Relative mRNA Expression
Unstim.
LPS
IL-4
1ng/mL IL-10
10ng/mL IL-10
IL4 + 1ng/mL IL-10
IL4 + 10ng/mL IL-10
F
Arginase Activity
Activity (units/ L)
Unstim.
IL-4
IL-10
IL-4+IL-10
G
Arg1
Relative mRNA Expression
4get/KN2. TWT sup.
4get/KN2. TΔBcl6 sup.
Rat IgG
αIL-10R
H
BMDMs
Unstim.
IL-4
IL-10
IL-4 + IL-10
PD-L2
PD-L2 MFI of BMDMs
I
Unstim.
IL-4
IL-10
IL-4 + IL-10
5.2
30
5.6
11
FSC-H
MHC-II
% MHC-II+ of BMDMs
J
Unstim.
IL-4
IL-10
IL-4 + IL-10
16
55
2.0
2.7
CD4
CFSE
% proliferating OT-II cells
K
OT-II cells
Unstim.
IL-4
IL-10
IL-4 + IL-10
CD44
% CD44+ OT-II cells
L
OT-II cells
Unstim.
IL-4
IL-10
IL-4 + IL-10
CD25
% CD25+ OT-II cells

Foxp3$^-$CD4$^+$ T cells expressed significantly more Blimp-1, while there was no change in expression by Foxp3$^+$ Treg cells (Figs. 2D and 2E). Consistently, there was a greater frequency of IL-10-producing CD4$^+$ T cells in the gut-draining mesLNs from days 5 (the initiation of detectable T cell priming) to 14 (the peak of the CD4$^+$ T cell response) post-infection (Fig. 2F)[4]. Notably, *Hpb* infection was required to elicit differences in IL-10 production, as we found minimal cytokine secretion by CD4$^+$ T cells from either genotype under uninfected conditions (Supplementary Figs. 1A and 1B). Taken together, these results indicate that Bcl-6 negatively regulates the expression of Blimp-1 and IL-10 by CD4$^+$ T cells during *Hpb* infection.

Recently, the Blimp-1/Bcl-6 axis has been demonstrated to regulate the production of IL-10 by Th2 cells in a model of allergen-induced asthma[18]. Because we observed that Bcl-6 constrained the expression of Blimp-1 and IL-10, we tested whether Bcl-6 would also limit IL-10 production by Th2 cells during helminth infection. First, we assessed IL-10 production by *in vitro*-differentiated CD4$^+$ T effector cells. Following culture of Bcl-6-deficient and -sufficient naive CD4$^+$ T cells under Th2 or Th1 polarizing conditions, we first noted that Th2 cells secreted close to four times more IL-10 compared to their Th1 counterparts (Fig. 2G). Furthermore, Bcl-6-deficient CD4$^+$ T cells, regardless of culture conditions, produced significantly more IL-10 compared to Bcl-6-sufficient T cells (Fig. 2G). Thus, Bcl-6 can limit the production of IL-10 by diverse effector lineages of CD4$^+$ T cells *in vitro*.

CD4$^+$ T cells are a significant source of IL-10 during *Hpb* infection[6]. Therefore, we evaluated if Bcl-6 would suppress the production of IL-10 by either Gata-3$^+$ Th2 or Foxp3$^+$ Treg cells, the most abundant CD4$^+$ T cell effector subsets after *Hpb* infection. Indeed, both activated CD4$^+$Gata-3$^-$ and CD4$^+$Gata-3$^+$ T cells from the meLN produced IL-10 at 14 days post-infection after *in vitro* restimulation. While there was no change in the frequency of CD4$^+$Gata-3$^-$IL-10$^+$ cells, there were significantly more Gata-3$^+$ Th2 cells producing IL-10 (Fig. 2H). No significant changes in the frequency of activated CD4$^+$Foxp3$^+$IL-10$^+$ Tregs were observed (Fig. 2I). Collectively, these data support our hypothesis that Bcl-6 limits the production of IL-10 by Th2 cells during helminth infection.

Elevated production of IL-10 by Th2 cells in 4get/KN2.T$^{\Delta Bcl6}$ mice may be an indirect effect of the loss of GCs and atypical lymph node architecture. To determine if the elevated IL-10 production is a direct result of Bcl-6 deficiency in CD4$^+$ T cells, we assessed IL-10 production by Th2 cells in 4get/KN2.B$^{\Delta Bcl6}$ mice. The frequency of IL-10-producing CD4$^+$CD44$^+$Gata3$^+$ Th2 cells was unchanged after intrinsic deletion of Bcl-6 in the B cell compartment (Fig. 2J). Thus, IL-10 production by CD4$^+$ T cells is not altered by a defective GC response. As an alternative approach and to confirm if Bcl-6 influences IL-10 production by Th2 cells in the presence of GCs and Tfh cells, bone marrow chimeras were created where αβ T cell-deficient CD45.1$^+$ lethally irradiated recipients received equal amounts of CD45.1$^+$ wildtype and either CD45.2$^+$ Bcl-6$^{fl/fl}$ or Rosa26-Ert2creBcl-6$^{fl/fl}$ bone marrow cells. Rosa26-Ert2cre mice express a tamoxifen-inducible Cre recombinase under control of the ubiquitously expressed Rosa26 locus[23], allowing the temporal deletion of Bcl-6 in all donor cells expressing Cre recombinase. Generation of these chimeras enables us to test the relevance of Bcl-6 expression in the CD4$^+$ T cell compartment in the presence of a Tfh cell-dependent GC response. It also obviates any impact that Bcl-6 may have during T cell development. After 12 weeks of reconstitution, mice were treated with tamoxifen and infected with *Hpb* 7 days later. While there was a nonsignificant increase in the ratio of IL-10$^+$ Gata3$^-$CD4$^+$ T cells between Rosa26-Ert2creBcl-6$^{fl/fl}$ and Bcl-6$^{fl/fl}$ controls, we observed a significantly greater proportion of Rosa26-Ert2creBcl-6$^{fl/fl}$ Gata3$^+$ Th2 cells produced IL-10 at 14 days post-infection compared to controls (Fig. 2K). Therefore, Bcl-6 acts in a post-developmental, T cell-intrinsic manner to limit IL-10 production by Th2 cells.

Fig. 4 IL-10 synergistically enhances IL-4-mediated alternative activation of macrophages. (A–D) 4get/KN2.T$^{\Delta WT}$ and 4get/KN2.T$^{\Delta Bcl6}$ mice were infected with 200 L3 *Hpb* larvae by gavage and treated every third day from the onset of infection with Rat IgG or anti-IL-10R blocking antibody. MesLNs or duodenal tissue were harvested at 2 weeks postinfection unless indicated otherwise. Cells were isolated by digesting tissue for 30 minutes with collagenase IV. (A) Representative frequencies and the total number of CD206$^+$CD64$^+$Ly6C$^-$Ly6G$^-$Siglec-F$^-$CD11b$^+$-CD3$^-$B220$^-$ mesLN cells. (B) Mean fluorescent intensity (MFI) of CD206 by CD64$^+$Ly6C$^-$Ly6G$^-$Siglec-F$^-$CD11b$^+$CD3$^-$B220$^-$ mesLN cells. (C) MFI of PD-L2 by CD64$^+$Ly6C$^-$Ly6G$^-$Siglec-F$^-$CD11b$^+$CD3$^-$B220$^-$ cells isolated from mesLNs or the small intestine. (D) Representative images of RNAscope for *Arg1* mRNA in duodenal sections from 2-week *Hpb*-infected mice. (E–L) BMDMs from C57BL/6 mice were stimulated with LPS (50 ng/ml), IL-4 (10 ng/ml), and IL-10 (10 ng/ml) unless otherwise stated for 24 hours. (E) mRNA expression levels of *Arg1* normalized to *Hprt* relative to unstimulated controls. (F) Stimulated BMDMs were lysed, and an arginase activity assay was performed. (G) Naive CD4$^+$ T cells were isolated from the peripheral lymph nodes of 4get/KN2.T$^{\Delta WT}$ and 4get/KN2.T$^{\Delta Bcl6}$ mice and stimulated under Th2-polarizing conditions (5 ng/ml IL-2, 10 ng/ml IL-4, and 1 mg/ml anti-IFNγ) with anti-CD3/28. After 96 hours of stimulation, supernatant was collected. BMDMs were stimulated with 25% T cell supernatant in addition to 10 mg/ml of anti-IL-10R antibody (clone 1B1.3A) or isotype control. mRNA expression levels of *Arg1* were assessed after 24 hours of BMDM stimulation normalized to *Hprt* relative to unstimulated controls. (H) PD-L2 MFI representative histogram and quantification by flow cytometry of BMDMs. (I) Representative contour plots of MHC-II expression by BMDMs following the indicated stimulation. (J–L) Macrophages were stimulated as indicated and pulsed with whole chicken ovalbumin for 24 hours prior to washing and coculture with CFSE-labeled OT-II lymphocytes for 72 hours. (J) Representative contour plots and quantification of CFSE dilution to indicate OT-II T cell proliferation. Representative histograms and quantification of CD44 (K) and CD25 (L) expression by OT-II T cells cultured with BMDMs stimulated as indicated. (E, H) Compiled from two independent experiments with at least three mice per group. (A–D, F, G, and I–L) Representative of at least two independent experiments with four mice per group. (B and C) Data analyzed by two-tailed Student's t test. (A and E–L) One-way ANOVA was performed for statistical analysis. Dots in graphs represent individual mice. ***$p < 0.001$, **$p < 0.01$, and *$p < 0.05$. ns, not significant. ANOVA = analysis of variance; BMDM = bone marrow-derived macrophage; *Hpb* = *Heligmosomoides polygyrus bakeri*; IFNγ = interferon γ; IL = interleukin; IL-10R = IL-10 receptor; LPS = lipopolysaccharide; mesLN = mesenteric lymph node; MFI = mean fluorescent intensity.

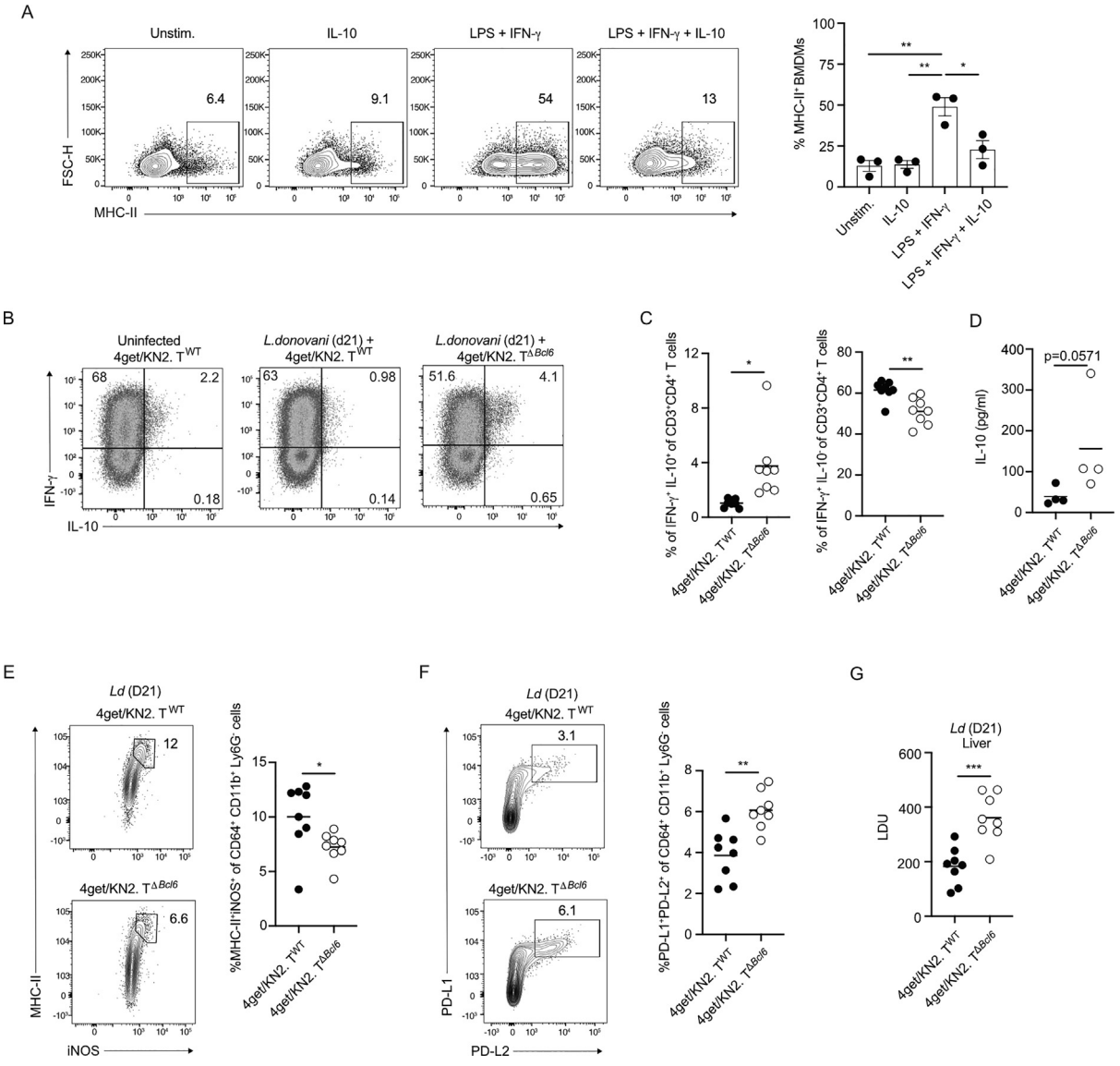

Fig. 5 Deletion of Bcl-6 in CD4$^+$ T cells enhances the generation of IL-10-producing Th1 cells and compromises resistance to visceral Leishmaniasis. (A) Representative contour plots and frequency of MHC-II expression by flow cytometry of BMDMs stimulated with LPS (50 ng/ml), IFNγ (10 ng/ml), and IL-10 (10 ng/ml) for 24 hours. (B–G) 5×10^5 total CD4$^+$ T cells were transferred from 4get/KN2.T$^{\Delta WT}$ or 4get/KN2.T$^{\Delta Bcl6}$ mice into *Rag1*$^{-/-}$ recipient mice. Recipients were infected with 4×10^7 amastigote *Leishmania donovani* 24 hours after transfer and sacrificed 3 weeks postinfection. (B and C) Cells were isolated from the liver and stimulated with phorbol myristate acetate (PMA) and ionomycin. Intracellular cytokine staining was performed 4 hours post-stimulation. Representative contour plots (B) and frequency (C) of IL-10 and IFNγ-producing CD3$^+$CD4$^+$ T cells. (D) Cells were isolated from the liver and cocultured with BMDCs previously pulsed with fixed *L. donovani* amastigotes for 6 hours at 37 °C. Concentration of IL-10 found in supernatant detected by ELISA. (E) Representative contour plots and frequency of liver CD45.2$^+$CD64$^+$CD11b$^+$Ly6G$^-$MHC-II$^+$iNOS$^+$ macrophages. (F) Representative contour plots and frequency of liver CD45.2$^+$-CD64$^+$CD11b$^+$Ly6G$^-$PD-L1$^+$PD-L2$^+$ macrophages. (G) Liver parasite burden. (A, B, and D) Representative of two independent experiments with at least three mice per group. (C and E–G) Compiled from two independent experiments with at least four mice per group. Dots in graphs represent individual mice. Data were analyzed by two-tailed Student's t test unless otherwise stated. One-way ANOVA was used in (A). ***$p < 0.001$, **$p < 0.01$, and *$p < 0.05$. ns, not significant. ANOVA = analysis of variance; BMDM = bone marrow-derived macrophage; ELISA = enzyme-linked immunosorbent assay; IFNγ = interferon γ; IL = interleukin; LPS = lipopolysaccharide; MHC II = major histocompatibility complex II; PMA = XXX; Th = T helper.

IL-10 signaling enhances type 2 cytokine-dependent goblet cell differentiation and *Hpb* expulsion

We next investigated the mechanism by which 4get/KN2.T$^{\Delta Bcl6}$ mice exhibited enhanced resistance to primary *Hpb* infection. Despite a robust endogenous type 2 immune response, adult *Hpb* worms are not efficiently expelled from the intestine, normally resulting in chronic infection[8]. However, amplification of type 2 cytokine signaling by administration of long-acting IL-4 complexes during the luminal stage of infection leads to *Hpb* expulsion during primary infection[9]. Furthermore, IL-10 produc-

tion by Th2 cells has been associated with host resistance to *Hpb*[24] and can compromise adult worm fecundity[6]. Thus, we hypothesized that increased IL-10 production by Bcl-6-deficient Th2 cells may locally amplify a key feature of epithelial-mediated worm expulsion, namely goblet cell differentiation. To test this hypothesis, we first determined that, similar to our mesLN results (Fig. 2), gut-infiltrating Th2 cells isolated from 4get/KN2.T$^{\Delta Bcl6}$ mice produced more IL-10 compared to Th2 cells from 4get/KN2.T^{WT} mice at 2 weeks post-infection (Fig. 3A). Consistent with these results, we observed an increase in activated STAT3 [phosphorylated STAT (pSTAT)3], a downstream target of IL-10 receptor signaling, within the small intestinal epithelium (Fig. 3B). To validate that intestinal epithelial cells are responsive to IL-10 as previously suggested[25], we isolated crypt cells from the duodenum of uninfected or day 14 *Hpb*-infected 4get/KN2.T$^{\Delta Bcl6}$ and 4get/KN2.T^{WT} mice and stimulated them *ex vivo* with recombinant IL-10. While crypt cells isolated from both groups of *Hpb*-infected mice had detectable STAT3 phosphorylation that was marginally increased upon IL-10 stimulation, uninfected crypts from 4get/KN2.T$^{\Delta Bcl6}$ mice were more responsive to IL-10 stimulation compared to crypts from uninfected 4get/KN2.T^{WT} controls (Fig. 3C). In contrast, we were unable to detect STAT3 activation following IL-10 stimulation of small intestinal organoid cultures generated from uninfected C57BL/6 mice despite robust induction of pSTAT3 following stimulation with our positive control, IL-22 (Supplementary Fig. 2A). We also did not observe a synergistic effect of IL-10 on type 2 cytokine (IL-4 or IL-13)-mediated induction of the goblet cell-associated protein Gob5 or goblet cell gene expression (e.g. *Muc2*, *Clca/Gob5*, and *Retnlb*) from these cultures, precluding us from further investigating the direct effects of IL-10 on epithelial cell differentiation (Supplementary Figs. 2B–2F). These data suggest that while the intestinal epithelium in 4get/KN2.T$^{\Delta Bcl6}$ mice may be more responsive to IL-10 signals *in vivo*, additional factors that license signaling of this cytokine are lost following *in vitro* culture.

To examine the potential functional implications of increased IL-10-producing Th2 cells, we counted duodenal goblet cells in uninfected mice as well as at two and 4 weeks post-*Hpb* infection. Although no difference in goblet cell frequency was detectable under uninfected conditions (Supplementary Fig. 2G), 4get/KN2.T$^{\Delta Bcl6}$ mice displayed a significant increase in goblet cell frequency relative to 4get/KN2.T^{WT} controls at 2 and 4 weeks post-infection (Figs. 3D and 3E). Goblet cell hyperplasia was IL-10-dependent, as antibody-mediated blockade of the IL-10 receptor (IL-10R)α subunit significantly decreased the number of goblet cells (Figs. 3D and 3E). Importantly, a decrease in goblet cell differentiation upon IL-10R blockade was associated with compromised worm expulsion in 4get/KN2.T$^{\Delta Bcl6}$ mice (Fig. 3F). In summary, Bcl-6 regulates the IL-10-dependent accumulation of goblet cells and increased expulsion of adult *Hpb* during primary infection, establishing this transcriptional repressor as a functional determinant of Th2-mediated anti-helminth immunity.

IL-10 synergistically enhances IL-4-mediated alternative activation of macrophages

Apart from driving worm expulsion, we sought to better understand how Th2-derived IL-10 in 4get/KN2.T$^{\Delta Bcl6}$ mice could be impacting other immune cellular networks. In addition to regulating the epithelial response, Th2 cells promote the accumulation of AAMs during helminth infection. These cells are commonly identified by their expression of CD206, PD-L2, and arginase-1, and have been shown to play varied roles in helminth infection, ranging from T cell suppression to driving expulsion during secondary infection[26,27]. While alternative activation of macrophages has been shown to be driven by Th2-cell-derived IL-4 or IL-13[26,28], studies have suggested IL-10 can augment this process[29]. Consistent with this finding, 4get/KN2.T$^{\Delta Bcl-6}$ mice displayed a striking increase in CD64^{+}CD206^{+} AAMs in the mesLNs at two weeks post-*Hpb* infection compared to infected 4get/KN2.T^{WT} mice (Fig. 4A). The accumulation of AAMs was IL-10 signaling dependent, as IL-10R blockade abrogated their increase following infection (Fig. 4A). Blockade of IL-10 signaling also decreased the Th2 response, exhibited by fewer CD4^{+}Gata3^{+} T cells, decreased frequencies of IL-4 (as determined by huCD2 reporter expression)[4] and IL-5-producing Th2 cells, and more interferon (IFN)γ-producing non-Th2 cells (Supplementary Fig. 3). No difference in AAM number was detectable under uninfected conditions (Supplementary Fig. 4A). In addition, we did not detect a difference between groups in the Mean fluorescent intensity of CD206 expression by CD64^{+} macrophages isolated from the mesLN or small intestine of either group (Fig. 4B). However, macrophages from 4get/KN2.T$^{\Delta Bcl6}$ mice upregulated the AAM marker PDL-2 in the mesLN and small intestine (Fig. 4C). Consistent with the presence of macrophages expressing an enhanced AAM phenotype within the SI, we observed an increase in arginase-1 transcripts in duodenal sections from 4get/KN2.T$^{\Delta Bcl6}$ mice within resolving *Hpb* granulomas by *in situ* hybridization (RNAscope; Fig. 4D). Overall, these results show that Bcl-6 repression of IL-10-dependent Th2 cell responses limits key features of macrophage alternative activation *in vivo*.

We next sought to assess the capacity of IL-10 to directly impact macrophage function in the context of a type 2 immune response. To this end, we generated bone marrow-derived macrophages (BMDMs) from C57BL/6 WT mice *in vitro* and measured expression of several markers of alternative activation after 24 hours of stimulation. While IL-10 alone did not induce expression of *Arg1*, it significantly enhanced IL-4-driven expression of this AAM-associated gene (Fig. 4E). Concordantly, arginase activity was significantly increased in BMDMs stimulated with a combination of IL-4 and IL-10, relative to those stimulated with IL-4 alone (Fig. 4F). IL-10 also enhanced IL-4 driven *Ccl24*, but not *Ym1* or *Retlna,* expression in BMDMs (Supplementary Fig. 4B). Cytokine stimulation of thioglycollate-induced peritoneal macrophages revealed a similar synergy between IL-4 and IL-10 on AAM-associated gene expression (Supplementary Fig. 4C). To test if Bcl-6-deficient Th2 cell products directly impacted macrophage activation, we stimulated BMDMs with supernatants from naive CD4^{+} T cells polarized under Th2 conditions *in vitro*. BMDMs stimulated with supernatants from *in vitro*-differentiated Bcl-6-deficient Th2 cells were found to express significantly higher levels of *Arg1* transcripts compared to those stimulated with supernatants from Bcl-6-sufficient Th2 cell cultures, an effect that depended on IL-10 signals (Fig. 4G). Altogether, these findings demonstrate that IL-10 is sufficient to directly augment IL-4-driven alternative macrophage differentiation.

Upon stimulation with IL-4, macrophages have been shown to upregulate processes promoting fatty acid oxidation, ultimately fueling an increase in mitochondrial oxidative phosphorylation[30]. This alteration of cellular metabolism is a key phenotypic change of AAMs, and studies have shown these modifications to be essential to the process of alternative activa-

tion[31]. We sought to assess if synergistic alterations to cellular metabolism would accompany the changes in gene expression observed in macrophages stimulated with IL-4 and IL-10. Analysis of macrophage bioenergetics found IL-10 and IL-4 to impart a modest increase in overall levels of oxygen consumption (a readout of oxidative phosphorylation) relative to IL-4 alone, while the extracellular acidification rate (a readout of glycolysis) remained unaffected (Supplementary Fig. 5). Analysis of metabolic sub-parameters showed that this trend was upheld, where dual cytokine stimulation had a modest but nonsignificant effect on cellular metabolism. In particular, spare respiratory capacity and maximal respiration appeared to be increased in IL-4/10-stimulated macrophages; however, relative to IL-4 alone, these increases did not reach statistical significance. Additionally, IL-10 stimulation alone appeared to induce minor metabolic changes to macrophages (Supplementary Fig. 5). Thus, IL-10 and IL-4 appear to have additive but not synergistic effects on AAM metabolism.

We next sought to assess other functional impacts that IL-10 could be imparting on AAMs, as these cells have been shown to inhibit T-cell responses during helminth infection through the expression of T cell inhibitory ligands such as PD-L2[32]. Consistent with *in vivo* findings, IL-4 and IL-10 synergistically induced high expression levels of PD-L2 relative to BMDMs stimulated with IL-4 alone (Fig. 4H). In line with the high expression of this T cell coinhibitory protein, we found that BMDMs stimulated with IL-4 alone upregulated the antigen presentation molecule major histocompatibility complex II (MHC-II), whereas the addition of IL-10 abrogated this upregulation (Fig. 4I). To determine if IL-10 stimulation could impair the capacity of macrophages to stimulate $CD4^+$ T cells, lymphocytes from OVA-specific OT-II mice were cocultured in the presence of OVA-loaded BMDMs previously stimulated with either IL-4, IL-10, or both. $CD4^+$ OT-II cells proliferated robustly if cocultured with unstimulated or IL-4-stimulated BMDMs. By contrast, BMDMs pre-stimulated with IL-10 or IL-10 and IL-4 failed to induce antigen-specific proliferation of $CD4^+$ OT-II cells (Fig. 4J). OT-II T cells cocultured with IL-4 and IL-10 stimulated BMDMs also failed to upregulate the activation markers CD25 and CD44 (Figs. 4K and 4L). Therefore, IL-10 imparts an immunomodulatory phenotype on macrophages in the presence of type 2 cytokines *in vitro* and *in vivo*.

Deletion of Bcl-6 in $CD4^+$ T cells enhances the generation of IL-10-producing Th1 cells and compromises resistance to visceral leishmaniasis

Thus far, we have demonstrated the capacity of Bcl-6 to limit IL-10 production by $CD4^+$ T cells and its impact on various components of a type 2-dominant immune response. However, *in vitro*-differentiated Bcl-6-deficient Th1 cells also produced more IL-10 (Fig. 2G), suggesting that Bcl-6 expression by $CD4^+$ T cells could also critically impact type 1 immune responses. The role of macrophages in host resistance to *Hpb* infection is dominant during secondary infection, where they sequester infectious larvae within granulomas in an antibody-dependent manner[12]. Therefore, primary *Hpb* infection is not an ideal setting to assess the impact of IL-10 on macrophage-mediated host resistance. By contrast, macrophages play an essential role in limiting the replication and clearance of the intracellular parasite *Ld*, a function significantly compromised by the presence of IL-10[33]. Moreover, MHC-II-restricted antigen recognition of infected macrophages by IFNγ-producing Th1 cells is required to drive parasite killing by inducible nitric oxide synthase (iNOS)-producing macrophages[34]. Consistent with this scenario, *in vitro* stimulation of BMDMs with lipopolysaccharide and IFNγ greatly elevated the expression of MHC-II, an effect that was reversed by the addition of IL-10 (Fig. 5A). Therefore, we hypothesized that increased production of IL-10 by Bcl-6-deficient $CD4^+$ T cells could limit MHC-II upregulation by macrophages *in vivo* and result in the failure to control *Ld* infection. To test this possibility, total $CD4^+$ T cells from 4get/KN2.$T^{\Delta Bcl6}$ or 4get/KN2.T^{WT} mice were transferred into *Rag1*$^{-/-}$ mice and infected intravenously with *Ld* to model visceral leishmaniasis. Three weeks post-infection, livers were harvested from recipient mice, immunophenotyping was performed, and parasite burden was quantified. Similar to results from our *Hpb* infection studies, donor Bcl-6-deficient $CD4^+$ T cells produced significantly more IL-10 following *in vitro* restimulation with PMA and ionomycin compared to control $CD4^+$ T cells (Figs. 5B and 5C). Notably, IL-10 production was largely restricted to IFNγ-producing Th1 cells, which were modestly but significantly decreased in the Bcl-6-deficient setting (Figs. 5B and 5C). More IL-10 was also detected in the supernatant of Bcl-6-deficient $CD4^+$ T cells restimulated in an antigen-specific manner with bone marrow-derived dendritic cells (BMDCs) pulsed with *Ld* amastigotes (Fig. 5D). There were also considerable changes in liver macrophages isolated from *Ld*-infected *Rag1*$^{-/-}$ mice that received Bcl-6-deficient $CD4^+$ T cells. Consistent with the ability of IL-10 to dampen MHC-II expression in the context of type 1 inflammatory signals *in vitro*, the frequency of hepatic MHC-II^+iNOS^+ macrophages was significantly diminished in mice receiving $CD4^+$ T cells derived from 4get/KN2.$T^{\Delta Bcl6}$ mice (Fig. 5E). Moreover, a greater frequency of liver macrophages co-expressed the coinhibitory molecules PD-L1 and PD-L2, but did not upregulate the AAM marker CD206 (Fig. 5F and Supplementary Fig. 6). In line with our immunophenotyping results, *Rag1*$^{-/-}$ mice that received Bcl-6-deficient $CD4^+$ T cells displayed a significant increase in liver parasite burden compared to mice that received Bcl-6-sufficient $CD4^+$ T cells (Fig. 5G). These data demonstrate that, in addition to intestinal helminth infection, Bcl-6 expression in $CD4^+$ T cells plays an important role in shaping the innate immune response and host defense against visceral *Ld* infection.

DISCUSSION

Evolutionary biologists have long proposed that asymptomatic yet persistent infections provide a benefit to pathogens by increasing their likelihood of transmission by long-lived hosts such as humans[35]. This form of host-parasite symbiosis can be facilitated by concomitant immunity, a state in which persistence of a pathogen promotes resistance to reinfection by the same pathogen, providing benefit to both host and parasite[36]. This concept may explain why helminth infection is one of the most prevalent asymptomatic infectious diseases worldwide. Understanding the mechanisms underlying the establishment of concomitant immunity may provide insight into resistance against parasitic helminth infections. While local remodeling of the intestinal epithelium has been attributed to promoting concomitant immunity to *Hpb*[37], the impact of the adaptive immune response has yet to be tested. Although the differentiation of $CD4^+$ T cells requires the integration of extensive transcriptional networks, we highlight the requirement of the transcriptional repressor Bcl-6 in establishing concomitant immunity. Enhancing Tfh cell-dependent *Hpb*-specific antibody responses to protect against reinfection, Bcl-6 concurrently promoted the chronicity of an existing adult worm population by limiting the

Th2 cell effector program. As Bcl-6 expression by $CD4^+$ T cells is beneficial to the adult life stages of *Hpb*, it would be of interest to examine the capacity of adult helminth-derived products to directly enhance Bcl-6 expression, as adult *Hpb*-derived products have previously been reported to impact $CD4^+$ T cell responses[38,39]. These dual yet contrasting roles of Bcl-6 in primary versus secondary infection provide new insight into how transcriptional networks shape host defense strategies against intestinal symbionts.

The transcriptional repressor Bcl-6 has been established as the master regulator of Tfh cell differentiation[13–15]. While elegant work has defined its impact on a litany of transcriptional networks, if or how Bcl-6 directly promotes Tfh differentiation or other $CD4^+$ T cell effector lineages remains unanswered[40]. Not only does our data affirm that Tfh cells are required for the development of protective anti-helminth antibody responses, but it also outlines a previously unrecognized role for Bcl-6 in influencing the effector functions of Th2 cells in the context of infectious disease. While Bcl-6 expression did not impact the secretion of the canonical type 2 cytokines IL-4, IL-5, and IL-13, Bcl-6 intrinsically restricted the expression of Blimp-1 and the production of IL-10 by Th2 cells. Based on the well-established relationship between Bcl-6 and Blimp-1, we speculate that Bcl-6 indirectly limits IL-10 production by repressing the expression of Blimp-1[41]. However, the ability of Bcl-6 to limit IL-10 production by $CD4^+$ T cells may be restricted to settings of chronic infection because deletion of this transcription factor in a model of house dust mite allergy showed no impact on cytokine secretion[18].

IL-10 was first described to be secreted by Th2 cells and named cytokine synthesis inhibitory factor for its ability to suppress the production of Th1-associated cytokines[42]. Since then, a focus on the important anti-inflammatory properties of IL-10 and its production by immunosuppressive $Foxp3^+$ Treg cells has overshadowed these original observations. However, the contribution of IL-10 to type 2 immunity has recently been revisited and shown to be a component of the Th2 response during diverse species of helminth infection[6,7]. Building on these observations, we demonstrate that a Bcl-6/IL-10 axis is determinant of host resistance to primary and secondary *Hpb* infection via distinct mechanisms. Interestingly, we did not detect a change in the ability of Bcl-6 to regulate the production of IL-10 in Treg cells. Since Bcl-6 is required to generate IL-10-producing T follicular regulatory cells, a subset of $Foxp3^+$ Treg cells that regulate humoral immunity[43], future studies should examine whether this transcriptional repressor modulates IL-10 production in this specific population.

Contrary to its immunoregulatory functions, we describe a role for Bcl-6-mediated IL-10 production by Th2 cells in enhancing type 2 immune responses during helminth infection. Bcl-6 expression by $CD4^+$ cells restrained helminth-induced type 2 immune-associated processes, including weep-and-sweep responses and AAM differentiation. Examination of the intestinal response in 4get/KN2.$T^{\Delta Bcl6}$ mice revealed that IL-10R signaling increased intestinal goblet cell differentiation and clearance of adult worms. While STAT3 is not exclusive to IL-10 signaling, our observation of elevated pSTAT3 levels in the duodenum of 4get/KN2.$T^{\Delta Bcl6}$ mice and following *ex vivo* stimulation of intestinal crypt cells with IL-10 is highly suggestive of direct IL-10 signaling in the intestinal epithelium. These results are also consistent with a recent study demonstrating that mice lacking the IL-10RA subunit fail to increase goblet cell differentiation and cannot clear primary infection of *Trichuris muris*, a cecal-dwelling helminth parasite[7]. However, it remains to be determined how IL-10 specifically impacts goblet cell biology, such as their differentiation or maintenance during helminth infection. Nevertheless, we cannot rule out the possibility that, in 4get/KN2.$T^{\Delta Bcl6}$ mice, Th2-derived IL-10 acts on an intermediate cell type that, in turn, produces another factor that stimulates type 2 cytokines responsible for changes to the epithelium.

In addition to the epithelial response, our study revealed that T-cell-derived IL-10 can regulate macrophage polarization and their antigen-presenting capacity. Our *in vitro* phenotyping studies found IL-10 to synergize with IL-4, inducing changes to alternative activation. One such striking change was the profound upregulation in *Arginase1* mRNA and protein activity upon BMDM being stimulated with IL-4 and IL-10. These results are in line with previous observations examining *Arginase1* mRNA in IL-4/10-stimulated peritoneal macrophages[44] and expand upon these studies, by demonstrating an increase in functional protein expression. Beyond serving as a marker of alternative activation, arginase-1 is also a rate-limiting enzyme in metabolic pathways of polyamine biosynthesis[45]. Polyamines have been shown to have direct larvicidal activity for polyamines against *Hpb*[12] as well as direct effects on the polarization of macrophages themselves[46]. Indeed, we also noted increased *Arginase1* expression in the small intestine of 4get/KN2.$T^{\Delta Bcl6}$ mice at sites of previous tissue invasion by *Hpb* larvae. As we only observed differences in adult worm burden or parasite fitness during the chronic stages of luminal infection (beginning at 4 weeks post-infection), we propose that the differences in host resistance are predominantly mediated by changes to the epithelial response. Consistently, previous studies have suggested that arginase-producing intestinal macrophages play a larger role in mediating larval damage during secondary infection, owing to the potentiating effects of Fc-mediated engagement of parasite-specific antibody that are lacking in the absence of Bcl-6 expression[12]. However, other studies have shown that enhanced AAM polarization correlated with decreased parasite burden during primary infection[24,47]. Thus, we cannot exclude the possibility that, in the current setting, mucosal macrophages impinge on parasite fitness during their tissue-dwelling stage in a way that we were only able to measure during luminal colonization.

In contrast to *Hpb* infection, deletion of Bcl-6 in $CD4^+$ T cells resulted in compromised host resistance to *Ld* infection. In this latter setting, Bcl-6-deficient T cells produced more IL-10 and less IFNγ during a type 1 inflammatory antiparasitic response, highlighting a multifaceted role for Bcl-6 in impacting Th1 cell biology as well. Although we observed the increased generation of $PDL\text{-}2^+$ immunoregulatory macrophages across infection settings, we propose a model in which the differentiation of immunoregulatory AAM, while contributing to type 2 immunity, also limits $CD4^+$ T cell activity. Thus, any potential direct anti-helminth activity (i.e. nutrient deprivation or parasite killing) mediated by AAM may be negated by their simultaneous inhibitory effects on Th2 activity at the site of infection. As a result, the net increase in worm expulsion mediated by IL-10 is largely due to its effects on the epithelial weep-and-sweep response. Studies involving cell type-specific deletion of IL-10 signaling would be required to address this idea. By contrast, host resistance to intracellular *Ld* absolutely requires Th1-mediated licensing of macrophages with killing capacity. In this setting, IL-10 compromises cognate T cell engagement with *Ld*-infected macrophages

and, in the absence of other host defense mechanisms, increases susceptibility. Collectively, our results emphasize how the impact of IL-10 depends on the infectious agent and the cell types involved in host resistance.

METHODS

Animals and *Hpb* Infections

Experiments not involving *Ld* were approved by the McGill University Animal Care Committee, and mice were used at 6–16 weeks of age. For experiments involving *Ld*, mice were housed at the INRS animal facility under specific pathogen-free conditions, used at 6–12 weeks of age, and were carried out under protocols approved by the Comité Institutionnel de Protection des Animaux of the INRS-Centre Armand Frappier Santé (1910-01, 2002-03). These protocols respect procedure on good animal practice provided by the Canadian Council on Animal Care. 4get/KN2, CD45.1^{+}*Tcrβ*$^{-/-}$, CD4cre, Mb1cre, Bcl6$^{fl/fl}$, OT-II. Thy1.1^{+}Rag1$^{-/-}$, and Rosa26.Ert2cre mice on a C57BL/6 background were bred and kept under specific pathogen-free conditions at McGill University. Mb1cre and Bcl6$^{fl/fl}$ mice were provided by Dr M. Reth (Max Planck Institute, Freiburg, Germany) and Dr T. Takemori (Riken Institute, Yokohama, Japan)[18], respectively.

Hpb infection

Mice were infected by gavage with 200 L3 *Hp* larvae and harvested at the indicated time points. For protection experiments, adult *Hpb* were eliminated 4 weeks postinfection with two doses of 100 mg/kg pyrantel pamoate and subsequently challenged with 200 larvae. For some experiments, mice were administered 250 µg of anti-IL-10RA/CD210 (1B1.3A) or rat IgG (BioXcell, Lebanon, NH, USA) intraperitoneally every 72 hours for various lengths of time post-Hpb infection.

Hpb Fecundity quantification

At least 0.2 g of feces was collected and vortexed in a 0.75–1 ml saturated sodium chloride solution. Suspensions were incubated at room temperature for 24 hours, followed by at least 6 days at 4 °C. Then, the top two layers were extracted and centrifuged at 4000 rotations per minute (rpm) for 5 minutes, supernatants were discarded, and egg pellets were resuspended in double-distilled water for counting. Eggs were counted among 10 ul strips.

Ld infections

Ld (strain LV9) was maintained by serial passage in B6.129S7-*Rag1*^{tm1Mom} mice. Amastigotes were isolated from the spleens of infected animals. Mice were infected by injecting 2×10^7 amastigotes intravenously via the lateral tail vein. Parasite burden in the liver was determined using methanol-fixed, Giemsa-stained tissue impression smears. Data are presented as number of parasites per liver or as Leishman Donovan Units[48].

HES-specific IgG1 enzyme-linked immunosorbent assays

HES was prepared as previously described[49]. To detect HES-specific IgG1, we coated 96-well flat-bottom plates with 1 mg/ml of HES protein and incubated at 4 °C overnight. Serum samples were subsequently added, and antibodies were detected using rat anti-mouse IgG1-Biotin (SB77E) and Streptavidin-HRP (Southern Biotech, Birmingham, AL, USA).

Small intestine lamina propria

All fat and Peyer's patches were removed from the first 10 cm of the small intestine. The tissue was then cut longitudinally and washed in cold Hanks' balanced salt solution (HBSS) + ethylenediaminetetraacetic acid (EDTA) buffer [5 mM EDTA, 10% fetal bovine serum (FBS), and 15 mM HEPES]. After cutting the tissue into 0.5–1 cm pieces, it was subsequently placed in 15 ml of HBSS + EDTA buffer and incubated at 37 °C, 250 rpm, for 20 minutes. After shaking, the tissue was filtered through a 100 µm filter to remove the epithelial cells, and this process was repeated a second time. The tissue was then washed twice with 15 ml of cold HBSS buffer (2% FBS and 15 mM Hepes), followed by centrifugation for 2 minutes at 1800 rpm at 4 °C. Tissue was then digested in 5 ml of digestion buffer [Roswell Park Memorial Institute (RPMI), 10% FBS, 15 mM HEPES, 100 U/ml of DNAse, and 200 U/ml of Collagenase 8] at 37 °C, 250 rpm for 30 minutes. The digestion was stopped with 35 ml of cold R10 buffer (RPMI, 10 FBA, 15 mM HEPES, 1% L-glut Pen/Strep, and 1% L-glutamine). Tissue was crushed, passed through a 100 µm filter, and centrifuged at 2500 rpm for 10 minutes at 4 °C.

Liver cell extraction

Livers from infected animals were perfused with sterile 1× phosphate buffer saline (PBS). Harvested livers were then cut into smaller pieces and digested using Collagenase D (Sigma-Aldrich, St. Louis, MI, USA) solution in RPMI for 45 minutes on a rotating wheel. Digested pieces were crushed, passed through a 70 µm cell strainer, and washed with sterile 1× PBS. Collected cells were centrifuged at 500 rpm for 5 minutes. Hepatocyte pellet was discarded, and the supernatant containing lymphocytes was transferred to a clean 50 ml tube. The supernatant was centrifuged at 1200 rpm for 7 minutes. The resulting pellet was resuspended in 40% Percoll (Sigma-Aldrich), slowly added to 70% Percoll to create a gradient, and centrifuged at 1700 rpm for 15 minutes at room temperature with no acceleration and no breaks. After the Percoll-gradient centrifugation, the ring of lymphocytes at the center was carefully collected and washed twice with sterile 1× PBS, and the cells were used for various experiments.

MesLN macrophage isolation

MesLNs were cut into small pieces and incubated for 1 hr at 37 °C in digestion buffer (RPMI, 10% FBS, 15 mM HEPES, 100 U/ml of DNAse, and 150 U/ml of Collagenase IV). Remaining tissue was subsequently strained and crushed through a 70 um filter, then centrifuged at 1500 rpm for 5 minutes at 4 °C to isolate mesLN cells.

Flow cytometry

Data were acquired with a FACS Canto II or LSR Fortessa (BD Biosciences, Franklin Lakes, NJ, USA) and analyzed using FlowJo software. Antibodies used include: B220 (RA3-6B2), CD3 (145-2C11), huCD2 (RPA-2.10), CD11b (M1/70), CD11c (N418), CD45.2 (104), CD45.1 (A20), CD62L (MEL-14), CD44 (IM7), CD25 (PC61.5), Gata3 (TWAJ), Foxp3 (FJK-16s), MHC-II (M5/144.15.2), IL-13 (eBio13a), IFNγ (XMG1.2), and F4/80 (BM8) were purchased from Thermo Fisher Scientific (Waltham, MA, USA). Blimp-1 (C-21), IL-10 (JES5-16E3). Siglec-f (E50-2440), iNOS (6/iNOS/NOS type II), were purchased from BD Biosciences. IL-5 (TRFK5), CD64 (X54-5/7.1), CD206 (C068C2), Ly6C (HK1.4), Ly6G (1A8), PDL2 (TY25), Ep-CAM (G8.8), and PD-L1 (10F.9G2) were purchased from BioLegend (San Diego, CA, USA). Fixable viability

dye (Thermo Fisher Scientific) was used to exclude dead cells. Staining for intracellular proteins was performed using reagents suggested by the manufacturers (Thermo Fisher Scientific or BD Biosciences). For Gob5 staining, cells were fixed with 4% paraformaldehyde (PFA) then primary antibody staining with anti-Gob5/Clca1 (EPR12254-88 from Abcam, Cambridge, United Kingdom) was performed in permeabilization buffer (Thermo Fisher Scientific). Secondary staining with Goat anti-rabbit-AF488 antibody (A-11008; Thermo Fisher Scientific) in permeabilization buffer.

Generation of bone marrow chimeras

Bone marrow cells from CD45.1$^{+/+}$ mice were mixed with either Bcl6$^{fl/fl}$ or Ert2.cre Bcl6$^{fl/fl}$ bone marrow cells at a 1:1 ratio, and 5×10^6 total cells were injected intravenously into lethally irradiated (900 rad split into two doses) CD45.1^{+}*Tcrβ*$^{-/-}$ hosts. Following 12 weeks of hematopoietic reconstitution, chimeric mice were infected with *Hpb* larvae and processed as described in Fig. 4.

Adoptive transfer of CD4$^+$ T cells

For *Hpb*-related experiments, total CD4$^+$ T cells were isolated from the mesLNs of 4get/KN2.T$^{\Delta WT}$ and 4get/KN2.T$^{\Delta Bcl6}$ mice 2 weeks post-Hpb infection. CD4$^+$ T cells were isolated using the EasySepTM Mouse Naive CD4$^+$ T Cell Isolation Kit or the EasySepTM Mouse CD4$^+$ T Cell Isolation Kit as per the manufacturer's protocol (STEMCELL, Vancouver, BC, Canada). Flow cytometric analysis confirmed CD4+ T cell purity to be >97% by this method. Cells were resuspended in PBS, and 4×10^6 cells were intravenously administered to 7-day infected C57BL/6-WT recipients. After 21 days post-transfer (28 days postinfection), mice were sacrificed, and worm burden and fecundity were assessed.

For *Ld*-related experiments, total CD4$^+$ T cells were isolated from peripheral and mesLNs of uninfected 4get/KN2.T$^{\Delta WT}$ and 4get/KN2.T$^{\Delta Bcl6}$ mice. CD4$^+$ T cells were isolated using the EasySepTM Mouse Naive CD4$^+$ T Cell Isolation Kit or the EasySepTM Mouse CD4$^+$ T Cell Isolation Kit as per the manufacturer's protocol (STEMCELL). Cells were resuspended in PBS, and 0.5×10^6 cells were intravenously administered to 7-day infected Rag1$^{-/-}$ recipients. Mice were infected with *Ld* 24 hours later.

T cell culture

Naive CD62L$^+$CD4$^+$ T cells from peripheral lymph nodes were isolated using the EasySep Mouse Naive CD4$^+$ T Cell Isolation Kit as per the manufacturer's protocol (STEMCELL). Cells were subsequently stimulated with plate-bound anti-CD3 1 μg/ml, anti-CD28 (2 μg/ml), and the following combination of cytokines: Th0: no cytokine; Th1: anti-IL-4 (1 μg/ml), IL-2 (5 ng/ml), IL-12 (10 ng/ml), and IFNγ (2 ng/ml); and Th2: anti-IFN- (1 μg/ml), IL-2 (5 ng/ml), and IL-4 (10 ng/ml). All antibodies were purchased from Thermo Fisher Scientific, while all cytokines were purchased from PeproTech (Rocky Hill, NJ, USA).

Small intestinal crypt isolation and organoid culture

Small intestines were harvested, flushed with PBS, and cut. Intestine pieces were rinsed with PBS and then incubated in 2 mM EDTA at 4 °C for 30 minutes with gentle agitation. Crypts were then released from the SI by vigorous shaking in 10 ml PBS and then strained through a 70-μm cell strainer. Isolated crypts were resuspended in 10 ml basal organoid medium [Advanced DMEM/F12 (Gibco, Billings, MT, USA), 10 mM HEPES (Gibco), 1× GlutaMAX (Gibco), and 1% penicillin/streptomycin (Gibco)]. Crypts were plated in 30 μl Matrigel (Corning) domes, and 500 μl of culture medium was added to each well. Organoids culture medium (ENR): basal organoid medium with the addition of N2 Supplement (1:100; Gibco), B27 Supplement (1:50; Gibco), 1 mM N-acetyl cysteine (NAC), 50 ng/ml recombinant EGF, in-house made R-spondin 1, and Noggin CM (1:50). Organoids were passaged every 5 days, and on the day of the second passage, organoids were stimulated as indicated.

Immunoblot

Total protein concentration of samples was assessed by protein quantification assay under the manufacturer's instructions. The lysates were then diluted in a 5× loading buffer and incubated at 100 °C for 5 minutes. Next, samples (5 μg of crypts total lysate or 10 μg for organoids) were separated by sodium dodecyl sulfate–polyacrylamide gel electrophoresis and transferred on polyvinylidene difluoride membranes by wet blotting. The membrane was blocked by 5% bovine serum albumin in 1×TBS/0.1 % Tween-20 (TBST) at room temperature for 1 hour and incubated in primary antibody [pSTAT3, catalog #9145], (Cell Signaling Technology, Danvers, MA, USA), diluted 1000-fold] overnight at 4 °C. Membrane was washed three times and incubated with a secondary antibody for 1 hour at room temperature. The blots were detected by the chemiluminescence light-detecting kit. The total loading control was performed using the STAT3 antibody (STAT3, catalog #9139, Cell Signaling Technology, diluted 1000-fold).

pSTAT3 immunohistochemistry

Immunohistochemistry for phosphorylated STAT3 (residue Tyr705) was performed on 5-um thick paraffin-embedded formalin-fixed duodenal tissue sections. Antigen retrieval was performed using a 1:10 dilution of 10× Citrate Buffer (Sigma). pSTAT3 (Tyr705, clone D3A7) Rabbit mAb (Cell Signaling Technology) was used as the primary antibody. The secondary antibody was Anti-Rabbit EnVision+ System-HRP (Dako, Glostrup, Denmark).

BMDM culture

For BMDM cultures, femurs from C57BL/6-WT mice were harvested and cleared of surrounding muscle in cold PBS. Bone marrow cells were flushed in nondifferentiating media (RPMI 1640 containing 10% FBS and 1% penicillin/streptomycin) and centrifuged at 1800 rpm for 5 minutes at 4 °C. Red blood cells were lysed with 1× Red Blood Cell Lysis Buffer for 2–3 minutes, washed, and resuspended. $5–10 \times 10^6$ bone marrow cells were seeded in a 10 cm Petri Dish containing 15 ml of differentiating media (RPMI 1640 containing 10% FBS, 1% penicillin/streptomycin, and 20% L929 Cell Conditioned Medium). On the 3rd day of culture, dishes were supplemented with 10 ml of differentiating media. On the 6th day of culture, differentiated BMDMs were washed with PBS several times, detached using Cell Stripper, and plated in the desired format for stimulation in nondifferentiation media. Cells were allowed to adhere overnight prior to stimulations. To obtain L929 Cell Conditioned Medium media, L929 fibroblasts were cultured in L929 cell media (RPMI 1640 containing 10% FBS, 1% penicillin/streptomycin, and 1% L-glutamine). Cells were passaged up to T75 flasks and left in culture for 2–4 weeks. Afterward, media was collected, centrifuged, and subjected to 0.2 μm filtration before storage at −20 °C and used in BMDM cultures. For BMDM and OT-II cell cocultures, 800,000 BMDMs were stimulated as previously

described and then pulsed for 5 hours with OVA peptide. Following stimulation, 800,000 CFSE-labeled lymphocytes from OT-II^{+}Thy1.1$^{+/+}$*Rag1*$^{-/-}$ mice were added to wells containing BMDMs and cocultured for 72 hours.

Arginase1 RNAscope

In situ hybridization for arginase1 was performed on 5 um thick paraffin-embedded formalin-fixed duodenal sections using RNAscope 2.5 HD Assay – BROWN kit (Advanced Cell Diagnostics, Newark, CA, USA), with probe for Mm-arginase1 (reference 403431), according to the manufacturer's instructions.

Arginase activity assay

Arginase activity of BMDMs was assessed using the Arginase Activity Assay Kit (Sigma). 1.5×10^6 BMDMs were stimulated in 6-well plates with the indicated cytokines (10 ng/ml IL4, 10 ng/ml IL-10, or both) for 24 hours. After the stimulation period, cells were washed with PBS and lysed in fresh protein lysis buffer, and cell lysates were assayed for arginase activity according to the manufacturer's instructions. One unit of arginase is the amount of enzyme that will convert 1.0 mmol of L-arginine to ornithine and urea per minute at pH 9.5 and 37 °C.

Bioenergetic flux analyzer (Seahorse) assay

C57BL/6 BMDMs were seeded in 96-well plates from Seahorse Biosciences (Agilent Technologies, Santa Clara, CA, USA), at 100,000 cells/well. Cells were incubated at 37 °C 5% carbon dioxide overnight in RPMI 1640 containing 10% FBS and 1% penicillin/streptomycin. Cells were stimulated the following day with either 10 ng/ml IL-4, 10 ng/ml IL-10, or both, for 24 hours. After 24 hours, cells were washed and resuspended in Seahorse media. The Searhose Bioenergetic flux analyzer (Agilent Technologies) was used to measure the OCR and ECAR. Mitochondrial inhibitors were added in 10-minute intervals in the following order: oligomycin A (1.5 μM), FCCP (2 μM), and Antimycin A (2 μM).

Thioglycollate treatment

3% thioglycolate (DIFCO) was autoclaved and aged at room temperature for a minimum of 18 days (protected from light). The 1 ml of aged thioglycolate was administered intraperitoneally to mice. 96 hours postinjection, peritoneal lavage was performed with 10 ml of PBS. After isolation, peritoneal cells were plated in 24 well plates and rested for a minimum of 36 hours prior to stimulation.

Cytokine quantification

Cells (1.5×10^6) were stimulated in complete RPMI 1640 in the presence of 50 ng/ml PMA, 1 mg/ml ionomycin, and 0.67 mg/ml BD GolgiStop and/or Brefeldin A (BioLegend) for 4 hours. After stimulation, cells were stained as described above. For *Ld*-specific restimulation, single-cell suspensions of the liver were cocultured with BMDCs previously pulsed with fixed *Ld* amastigotes for 6 hours at 37 °C. Total IL-10 in supernatants was quantified using a mouse IL-10 enzyme-linked immunosorbent assay Ready SET-Go! kit (Thermo Fisher Scientific).

RNA sequencing and analysis

Total RNA from flow cytometry sorted CD4^{+}GFP^{+}CD44^{+}CXCR5^{-} cells at 2 weeks post-Hpb infection was obtained with Qiagen RNeasy Mini kit following the manufacturer's instructions. RNA was extracted using Trizol reagent (Sigma-Aldrich), and quality was checked with the Bioanalyzer RNA 6000 kit and sequenced using Novaseq 6000 sequencers (Illumina, San Diego, CA, USA). Raw reads are clipped for adapter sequence, trimmed for minimum quality (Q30) in 3′, and filtered for a minimum length of 32 base pairs using Trimmomatic[50]. Surviving read pairs were aligned to Mus_musculus assembly GRCm38 by the ultrafast universal RNAseq aligner STAR using the recommended two-passes approach[51]. Aligned RNA Seq reads were assembled into transcripts, and their relative abundance was estimated using Cuffflinks and Cuffdiff[52]. Differential expression was conducted using DEseq.

Quantitative polymerase chain reaction

mRNA was extracted using TRIzol (Sigma), and cDNA samples were prepared per manufacturer's protocol (Diamed, AD100-31404). Quantitative real-time reverse transcriptase polymerase chain reaction was performed using Advan Tech qPCR mix (Diamed, AD100-21402) on the Bio-Rad (Hercules, CA, USA) CFX96 Real-Time System and software. Fold expression was calculated using the $\Delta\Delta^{CT}$ method and *Hprt* as reference genes. Custom primers were generated for *Hprt*: forward (5′-AGGACCTCTC GAAGTGTTGG-3′), reverse (5′-AACTTGCGCTCATCTTAGGC-3′), *Arg1*: forward (5′-TGATGGAAGAGACCTTCAGC-3′), reverse (5′-CA CCTCCTCTGCTGTCTTCC-3′), *Retlna* (5′-TGCCAATCCAGCTAAC TATCC-3′), reverse (5′-CAGGCAGTTGCAAGTATCTCC-3′), *Ccl24* (5′-CCTCTGTCCCTGAACTTGGA-3′), reverse (5′-TCCCAGCTGGTCT GTCAAA-3′), *Ym1* (5′-CAGTGCCATGGTCTCTACTCC-3′), reverse (5′-AATGATTCCTGCTCCTGTGG-3′), *Muc2* (5′-ACCACAATCTC TACTCCCATCT-3′), reverse (5′-TCCAGTCAGACCAAAAGCAG-3′), *Clca1/Gob5* (5′-CTGTCTTCCTCTTGATCCTCCA-3′), reverse (5′-CGT GGTCTATGGCGATGACG-3′), Retnlb (5′-GATCAAGGAAGCTCT CAGTCG-3′), reverse (5′-TCC TCA TTC TTA AGC CAT TCG-3′) using Primer3 software.

Histology

All tissues were fixed with 10% formalin phosphate for at least 24 hours. After 24 hours, fixed tissue was briefly washed twice in PBS and transferred to 70% ethanol. Paraffin embedding and sectioning of tissue were performed by the Histology Core at the RI-MUHC. Select tissue sections were further stained with Periodic Acid Schiff or hematoxylin and eosin.

Statistical analysis

Data are expressed as mean ± SD. Data were analyzed by a two-tailed Student's t test or one-way analysis of variance as appropriate using the GraphPad Prism program (version 6). A p value <0.05 was considered significant.

AUTHOR CONTRIBUTIONS

Conceptualization: I.L.K. and A.P.M; Methodology: I.L.K., A.P.M., G. A.R., S.S., S.St., L.W., O.D.K., and A.G.; Investigation: A.P.M., G.A.R., S.S., L.W., E.P., D.K.A., D.R., A.R., and G.F.; Resources: J.N.M., M.D., O.D.K., A.G., S.St., and I.L.K.

DECLARATION OF COMPETING INTERESTS

The authors have no competing interests to declare.

FUNDING

This research did not receive any specific grant from funding agencies in the public, commercial, or not-for-profit sectors.

ACKNOWLEDGMENTS

The authors thank all members of the King laboratory for their support and feedback in preparing this manuscript. We greatly appreciate the technical support of Sarah Boissel (IRCM) for the RNA sequencing experiments, the MUHC-RI Animal Resource Division, and the Histology platform. This work was supported by the Canadian Institutes of Health Research (PJT-362757 to I. L.K. and PJT-159647 to S.St.). I.L.K. holds a Canada Research Chair in Barrier Immunity. A.P.M. holds a Human Frontiers Science Fellowship (LT000557/2020-L).

APPENDIX A. SUPPLEMENTARY MATERIAL

Supplementary material to this article can be found online at https://doi.org/10.1016/j.mucimm.2023.08.004.

References

1. Zhu, J., Yamane, H. & Paul, W. E. Differentiation of effector CD4 T cell populations (*). *Annu. Rev. Immunol.* **28**, 445–489 (2010).
2. Tuzlak, S. et al. Repositioning TH cell polarization from single cytokines to complex help. *Nat. Immunol.* **22**, 1210–1217 (2021).
3. Gowthaman, U. et al. Identification of a T follicular helper cell subset that drives anaphylactic IgE. *Science* **365**, eaaw6433 (2019).
4. Meli, A. P., Fontés, G., Leung Soo, C. & King, I. L. T follicular helper cell-derived IL-4 is required for IgE production during intestinal helminth infection. *J. Immunol.* **199**, 244–252 (2017).
5. Reinhardt, R. L., Liang, H. E. & Locksley, R. M. Cytokine-secreting follicular T cells shape the antibody repertoire. *Nat. Immunol.* **10**, 385–393 (2009).
6. Webster, H. C. et al. Tissue-based IL-10 signalling in helminth infection limits IFNgamma expression and promotes the intestinal Th2 response. *Mucosal Immunol.* **15**, 1257–1269 (2022).
7. Duque-Correa, M. A. et al. Exclusive dependence of IL-10Ralpha signalling on intestinal microbiota homeostasis and control of whipworm infection. *PLoS Pathog.* **15**, e1007265 (2019).
8. Reynolds, L. A., Filbey, K. J. & Maizels, R. M. Immunity to the model intestinal helminth parasite Heligmosomoides polygyrus. *Semin. Immunopathol.* **34**, 829–846 (2012).
9. Urban, J. F., Maliszewski, C. R., Madden, K. B., Katona, I. M. & Finkelman, F. D. IL-4 treatment can cure established gastrointestinal nematode infections in immunocompetent and immunodeficient mice. *J. Immunol.* **154**, 4675–4684 (1995).
10. Minutti, C. M. et al. Epidermal growth factor receptor expression licenses Type-2 helper T cells to function in a T cell receptor-independent fashion. *Immunity* **47**, 710–722.e6 (2017).
11. McCoy, K. D. et al. Polyclonal and specific antibodies mediate protective immunity against enteric helminth infection. *Cell Host Microbe* **4**, 362–373 (2008).
12. Esser-von Bieren, J. et al. Antibodies trap tissue migrating helminth larvae and prevent tissue damage by driving IL-4Ralpha-independent alternative differentiation of macrophages. *PLoS Pathog.* **9**, e1003771 (2013).
13. Johnston, R. J. et al. Bcl6 and Blimp-1 are reciprocal and antagonistic regulators of T follicular helper cell differentiation. *Science* **325**, 1006–1010 (2009).
14. Nurieva, R. I. et al. Bcl6 mediates the development of T follicular helper cells. *Science* **325**, 1001–1005 (2009).
15. Yu, D. et al. The transcriptional repressor Bcl-6 directs T follicular helper cell lineage commitment. *Immunity* **31**, 457–468 (2009).
16. Sawant, D. V. et al. Bcl6 controls the Th2 inflammatory activity of regulatory T cells by repressing Gata3 function. *J. Immunol.* **189**, 4759–4769 (2012).
17. Kusam, S., Toney, L. M., Sato, H. & Dent, A. L. Inhibition of Th2 differentiation and GATA-3 expression by BCL-6. *J. Immunol.* **170**, 2435–2441 (2003).
18. He, K. et al. Blimp-1 is essential for allergen-induced asthma and Th2 cell development in the lung. *J. Exp. Med.* **217**, e20190742 (2020).
19. Belkaid, Y., Piccirillo, C. A., Mendez, S., Shevach, E. M. & Sacks, D. L. CD4+CD25+ regulatory T cells control Leishmania major persistence and immunity. *Nature* **420**, 502–507 (2002).
20. Brunet, L. R., Kopf, M. A. & Pearce, E. J. Schistosoma mansoni: il-4 is necessary for concomitant immunity in mice. *J. Parasitol.* **85**, 734–736 (1999).
21. Hatzi, K. et al. BCL6 orchestrates Tfh cell differentiation via multiple distinct mechanisms. *J. Exp. Med.* **212**, 539–553 (2015).
22. Hollister, K. et al. Insights into the role of Bcl6 in follicular Th cells using a new conditional mutant mouse model. *J. Immunol.* **191**, 3705–3711 (2013).
23. Ventura, A. et al. Restoration of p53 function leads to tumour regression in vivo. *Nature* **445**, 661–665 (2007).
24. Filbey, K. J. et al. Innate and adaptive type 2 immune cell responses in genetically controlled resistance to intestinal helminth infection. *Immunol. Cell Biol.* **92**, 436–448 (2014).
25. Biton, M. et al. T helper cell cytokines modulate intestinal stem cell renewal and differentiation. *Cell* **175**, 1307–1320.e22 (2018).
26. Anthony, R. M. et al. Memory T(H)2 cells induce alternatively activated macrophages to mediate protection against nematode parasites. *Nat. Med.* **12**, 955–960 (2006).
27. Mantovani, A., Biswas, S. K., Galdiero, M. R., Sica, A. & Locati, M. Macrophage plasticity and polarization in tissue repair and remodelling. *J. Pathol.* **229**, 176–185 (2013).
28. Bosurgi, L. et al. Macrophage function in tissue repair and remodeling requires IL-4 or IL-13 with apoptotic cells. *Science* **356**, 1072–1076 (2017).
29. Makita, N., Hizukuri, Y., Yamashiro, K., Murakawa, M. & Hayashi, Y. IL-10 enhances the phenotype of M2 macrophages induced by IL-4 and confers the ability to increase eosinophil migration. *Int. Immunol.* **27**, 131–141 (2015).
30. Huang, S. C. et al. Cell-intrinsic lysosomal lipolysis is essential for alternative activation of macrophages. *Nat. Immunol.* **15**, 846–855 (2014).
31. O'Neill, L. A. & Pearce, E. J. Immunometabolism governs dendritic cell and macrophage function. *J. Exp. Med.* **213**, 15–23 (2016).
32. Huber, S., Hoffmann, R., Muskens, F. & Voehringer, D. Alternatively activated macrophages inhibit T-cell proliferation by Stat6-dependent expression of PD-L2. *Blood* **116**, 3311–3320 (2010).
33. Stäger, S. et al. Distinct roles for IL-6 and IL-12p40 in mediating protection against Leishmania donovani and the expansion of IL-10+ CD4+ T cells. *Eur. J. Immunol.* **36**, 1764–1771 (2006). https://doi.org/10.1002/eji.200635937.
34. Reiner, N. E., Ng, W., Ma, T. & McMaster, W. R. Kinetics of gamma interferon binding and induction of major histocompatibility complex class II mRNA in Leishmania-infected macrophages. *Proc. Natl Acad. Sci. U. S. A.* **85**, 4330–4334 (1988).
35. Brown, S. P. & Grenfell, B. T. An unlikely partnership: parasites, concomitant immunity and host defence. *Proc. Biol. Sci.* **268**, 2543–2549 (2001).
36. Råberg, L., Graham, A. L. & Read, A. F. Decomposing health: tolerance and resistance to parasites in animals. *Philos. Trans. R. Soc. Lond. B Biol. Sci.* **364**, 37–49 (2009).
37. Schneider, C. et al. A metabolite-triggered tuft cell-ILC2 circuit drives small intestinal remodeling. *Cell* **174**, 271–284.e14 (2018).
38. Johnston, C. J. C. et al. A structurally distinct TGF-beta mimic from an intestinal helminth parasite potently induces regulatory T cells. *Nat. Commun.* **8**, 1741 (2017).
39. Valanparambil, R. M. et al. Production and analysis of immunomodulatory excretory-secretory products from the mouse gastrointestinal nematode Heligmosomoides polygyrus bakeri. *Nat. Protoc.* **9**, 2740–2754 (2014).
40. Crotty, S. T follicular helper cell differentiation, function, and roles in disease. *Immunity* **41**, 529–542 (2014).
41. Crotty, S., Johnston, R. J. & Schoenberger, S. P. Effectors and memories: Bcl-6 and Blimp-1 in T and B lymphocyte differentiation. *Nat. Immunol.* **11**, 114–120 (2010).
42. Fiorentino, D. F., Bond, M. W. & Mosmann, T. R. Two types of mouse T helper cell. IV. Th2 clones secrete a factor that inhibits cytokine production by Th1 clones. *J. Exp. Med.* **170**, 2081–2095 (1989).
43. Laidlaw, B. J. et al. The Eph-related tyrosine kinase ligand ephrin-B1 marks germinal center and memory precursor B cells. *J. Exp. Med.* **214**, 639–649 (2017).
44. Van de Velde, L. A. et al. T cells encountering myeloid cells programmed for amino acid-dependent immunosuppression use Rictor/mTORC2 protein for proliferative checkpoint decisions. *J. Biol. Chem.* **292**, 15–30 (2017).
45. Monticelli, L. A. et al. Arginase 1 is an innate lymphoid-cell-intrinsic metabolic checkpoint controlling type 2 inflammation. *Nat. Immunol.* **17**, 656–665 (2016).
46. Latour, Y. L., Gobert, A. P. & Wilson, K. T. The role of polyamines in the regulation of macrophage polarization and function. *Amino Acids* **52**, 151–160 (2020).
47. Puleston, D. J. et al. Polyamines and eIF5A hypusination modulate mitochondrial respiration and macrophage activation. *Cell Metab.* **30**, 352–363.e8 (2019).
48. Bankoti, R. & Stäger, S. Differential regulation of the immune response in the spleen and liver of mice infected with Leishmania donovani. *J. Trop. Med.* **2012**:639304.

49. Meli, A. P. et al. The integrin LFA-1 controls T follicular helper cell generation and maintenance. *Immunity* **45**, 831–846 (2016).
50. Bolger, A. M., Lohse, M. & Usadel, B. Trimmomatic: a flexible trimmer for Illumina sequence data. *Bioinformatics* **30**, 2114–2120 (2014).
51. Dobin, A. et al. STAR: ultrafast universal RNA-seq aligner. *Bioinformatics* **29**, 15–21 (2013).
52. Trapnell, C. et al. Differential analysis of gene regulation at transcript resolution with RNA-seq. *Nat. Biotechnol.* **31**, 46–53 (2013).